A Multi-Index Investigation of the Spatiotemporal Relationships Between Heat and EMS Calls During the 2015 Pan American Games in Toronto, Canada

by

Alexandria J. Herdt, B.S.

A Thesis

In

Atmospheric Science

Submitted to the Graduate Faculty
of Texas Tech University in
Partial Fulfillment of
the Requirements for
the Degree of

MASTER OF SCIENCE

Approved

Dr. Guofeng Cao
Committee Chair

Dr. Jennifer Vanos

Dr. Robert Brown

Mark Sheridan
Dean of the Graduate School

August, 2017

ACKNOWLEDGEMENTS

I'd like to first and foremost thank my adviser Dr. Jennifer Vanos for her invaluable help provided throughout the thesis process. Her guidance and knowledge has been a major factor in my ability to excel here at Texas Tech over the years. I graduate as a better writer, researcher, and scientist because of the drive and passion she has inspired within me. For all of this, I thank her.

Secondly, I would like to thank Ian Scott-Fleming for all of his help with coding, insights and experience, and guidance throughout the completion of this thesis. His help in handling the unexpected roadblocks I encountered with data processing was crucial to the completion of my master's thesis.

I would also like to thank the other members of my thesis committee, Dr. Guofeng Cao and Dr. Robert Brown − not only for their time and constructive advice, but for their intellectual contributions to my development as a scientist. Their wisdom was sincerely appreciated along the thesis completion journey.

Additionally, the assistance of Melissa MacDonald and Dave Henderson of Environment Canada, Chris Olynyk of Toronto EMS, and Dr. Marc Lochbaum of TTU, in providing the necessary mesonet monitoring network data, EMS data, and athlete data was most appreciated. Again, without their assistance the completion of this thesis would not have been possible.

I wish to sincerely thank Matthew Brothers for being a source of great emotional support throughout my entire graduate school experience. His endless encouragement, patience, and reminders to take breaks to enjoy life were also critical in the success of my thesis project. I cannot adequately express how thankful I am to have had him as a best friend through this journey.

To my parents and my Oma and Opa, thank you for always encouraging me to

be an independent thinker and having confidence in my ability to go after new things that inspire me. I am the strong, outspoken, and driven women I am today because of everything you have urged me to try. Thank you for your constant support through the ups and downs of my academic career. It has been bumpy at times, but your belief in me has enhanced my ability to get through it all and succeed in the end. I'd also like to thank all of my relatives and friends who were there to listen, offer supporting words, and help me laugh away my stresses over the research and thesis writing process. You all mean the world to me.

Last but certainly not least, thank you to my younger siblings, Torie and Christian. To be a role model for you two is what has always fueled my ambition and pushed me to always strive to do better. Thank you for your unwavering support and for being my biggest fans. This thesis is dedicated to you.

TABLE OF CONTENTS

ABSTRACT

Weather has a profound effect on human health and well-being, with extreme heat being one of the greatest causes of human morbidity, specifically at large gatherings such as sporting events. Various univariate, bivariate, and multivariate heat stress metrics are used to identify episodes of oppressive weather that are detrimental to human health. In an attempt to better understand weather variations in the Greater Toronto Area (GTA), Environment Canada deployed a mesonet system of 53 weather stations during the summer of 2015 during which the Pan American Games were held and where thousands of tourists and athletes visited Toronto. This research combines the mesonet data with pin-pointed EMS ambulance response data, which allows for a unique and detailed exploration of the effects of heat on human health than is traditionally possible with city-wide weather and health estimates.

The goal of the current study is therefore to investigate the relationship between various heat stress metrics and heat illness in Toronto, Canada during the summer of 2015. Spatiotemporal analyses are completed through statistical comparisons between five heat stress metrics: daily temperature: maximum (T_{max}) and minimum (T_{min}), humidex, wet-bulb globe thermometer index, and the COMFA human energy budget (EB) model. All metrics were also compared to heat-related (HR) EMS calls for three human spatial exposure proxies (airport, averaged-city, and station-specific). With these heat metrics and the health data, the following tasks/objectives were pursued: create heat metric-based spatial maps of the GTA, determine which heat metric and spatial exposure proxy has the strongest relationship with HR EMS calls, and perform human EB case studies during the Pan American Games' sporting events at venues of escalated risk of exposure.

Geospatial maps across the GTA demonstrate variations by heat metric, identifying Hamilton, Ontario as an area of escalated risk for HR illness. Additionally, statistical regression modeling of the human spatial exposure proxies and the heat stress metrics demonstrated that the more localized proxy (station-specific) and the COMFA heat metric had the strongest relationships with HR EMS calls within the city limits. A case study focused on thermal comfort at the Pan American Games' soccer venue (located in Hamilton) found that athlete and spectator EBs routinely reached the 'dangerous' level of experiencing heat stress, which aligned primarily with absorbed radiation and metabolic activity values.

These results provide new information on the potential benefits and uses of mesonet systems during large-scale events specific to extreme heat assessments. Findings improve our understanding of the variability among common heat metrics in relation to intra-urban heat-health burden to enhance Toronto's resilience to extreme heat. This information can be used to inform public health officials and/or urban planners alike of areas of increased heat exposure at a finer intra-urban scale, thereby creating awareness of the most crucial areas and times in which to implement corrective bioclimatic design and/or plan EMS dispatches/resources to on days of excessive heat.

LIST OF TABLES

LIST OF FIGURES

LIST OF ABBREVIATIONS

e.g.

C - Celsius

CI - Condfidence Interval

COMFA - Comfort Formula

EB - Energy budget

EMS - Emergency Medical Service

GTA - Greater Toronto Area

HR - Heat-related

K - Kelvin

LCZ - Local Climate Zone

LST - Local Standard Time

M_{act} - Metabolic activity

MET - Metabolic intensity

MPDS - Medical Priority Dispatch System

MSC - Meteorological Service of Canada

NHR - Non-heat-related

OLS - Ordinary Least Squares

R_{abs} - Absorbed radiation

RH - Relative Humidity

T_a - Air temperature

TC - Thermal Comfort

T_c - Core body temperature

TEMS - Toronto Emergency Medical Services

T_{max} - Maximum air temperature

T_{min} - Minimum air temperature

UHI - Urban Heat Island

V_a - Activity velocity

V_w - Wind speed

WBGT - Wet-Bulb Globe Thermometer

CHAPTER 1
INTRODUCTION

1.1 Pan and Para Pan American Games

The Pan American Games are an Olympic-style competition, held every four years in the year preceding the Summer Olympic Games for athletes from countries within the Americas. The Parapan American Games are a similar competition held immediately after the Pan American Games for athletes with physical disabilities. The two competitions combined will henceforth be referred to as the 'Games'. The major sporting event features a variety of summer sports competitions analogous to those found in the Summer Olympics. The most recent Games event took place in Toronto, Ontario, Canada in 2015 from July $10^{\text{th}} - 26^{\text{th}}$ and August $7^{\text{th}} - 15^{\text{th}}$, respectively. As with any summer sporting event, heat-related (HR) illnesses and deaths are always a risk (Eichner, 2002). Thus, monitoring and relaying real-time information regarding the physical environment during competitions is pivotal for athlete and spectator health-security.

1.2 Heat and Human Health

Weather has a direct and profound effect on human health and comfort, with heat being one of the greatest causes of mortality and morbidity (CDC, 2015). When functioning normally, the human body uses several mechanisms to regulate the generation and conservation of heat to maintain a core body temperature (T_c) of approximately 37°C (Bassil et al., 2009). However, participating in vigorous exercise and/or exposure to hot environmental conditions can overwhelm these mechanisms and cause a person to experience heat stress (Brotherhood, 2008). As extreme heat is proposed to remain the deadliest of all extreme-weather-related hazards in the

United States (Sheridan et al., 2009), there is a growing concern about the likelihood that warmer climates and increased heat wave frequency, intensity and duration brought about by anthropogenic climate change will enhance adverse health burdens on cities (Meehl and Tebaldi, 2004; Harlan and Ruddell, 2011).

Compared to surrounding rural areas, air temperatures (T_a) in cities are normally elevated due to the urban heat island (UHI) effect. The UHI effect can be a powerful force in city-scale and microscale climates through the combined impacts of high thermal mass (due to the absorptive properties of building and ground materials), inhibited ventilation (due to tall buildings), and heat emitted from vehicles and buildings (Luber and McGeehin, 2008). The UHI effect is most prominent overnight, raising the nighttime minimum temperature (T_{min}) up to 12°C on calm clear nights compared to rural areas (Oke, 1987). A heightened overnight T_{min} provides minimal relief from daytime heat stress, which has been correlated with excess HR illnesses and deaths of urban inhabitants (McGeehin and Mirabelli, 2001; Zhang et al., 2012). Continued rapid urbanization of cities will only expand the UHI effect and increase the number of people exposed to the health risks induced by urban heating.

Although all HR deaths and illnesses are avoidable, many people succumb to extreme heat every year. Having a city-wide public health response plan to heat is key for lessening health impacts. Bassil et al. (2009) express that understanding the geographical distribution of high-risk populations and regions within cities during episodes of hot weather is essential knowledge for public health officials. For example, if vulnerable locations and populations are spatially identified, those areas can be specifically targeted for increased emergency medical service (EMS) attention to reduce HR morbidity and mortality.

1.2.1 Heat-Health Impacts in Mid-Latitude Cities

Heat-health studies focused on northern cities and countries have become more common in recent years as modeling of future thermal environments has revealed that populations in mid-latitude cities are likely to experience the greatest increases in thermal stress (Jendritzky and Tinz, 2009) in response to climate change. This increase will be most pronounced in the summer when the two weather types (dry tropical and moist tropical) associated with HR mortality are present in the mid-latitudes (Sheridan and Kalkstein, 2004). The most sensitive mid-latitude regions are those where extremely high T_a occur infrequently (McGeehin and Mirabelli, 2001), such as many cities in southern Canada, where residents are less acclimatized to extremely warm environments.

When looking at the mortality risk of residents during heat waves in 43 United States communities, Anderson and Bell (2011) found that northeast cities reported the strongest association with relative risk of mortality. Similarly, in a comparative climate analysis of HR EMS dispatches in Chicago and Phoenix completed by Hartz et al. (2013), it was found that the number of HR EMS dispatches in both cities climbed rapidly with increasingly high temperatures, however the threshold at which this climb occurred was much lower in Chicago, with a steeper response. Accordingly, mid-latitude cities are important to study as their residents are just as susceptible to the health impacts of heat but may react differently due to the absence of cooling shelters in public areas (Luber and McGeehin, 2008), unawareness of modifications in activities or increased air conditioning use crucial for coping with the heat (Kinney et al., 2008), and being less acclimated to high temperatures (Kalkstein, 2000).

1.2.2 Human Vulnerability to Heat Stress

At an intra-urban scale, many studies have focused on identifying the most heat-vulnerable members of a city's population (Harlan et al., 2006; Hondula et al., 2012; Johnson et al., 2012). Many studies further find that HR mortality is highest amidst young children, elderly, individuals with pre-existing illness, low-income and less-educated groups, and minorities, with considerable differences across gender and race (Smoyer-Tomic and Rainham, 2001; Hajat and Kosatky, 2010; Hansen et al., 2011; Yardley et al., 2011; Reid et al., 2009, Uejio et al., 2011). During hot weather exposure, many individual characteristics influence who will be affected, either for physiological or behavioral reasons (Kinney et al., 2008). Although important, the multiplicity of these characteristics often causes other vulnerable populations to be overlooked. Athletes, attendees at a mass gathering, and tourists are three specific subsets of a population that can be negatively affected during episodes of hot weather as well because they are more likely to be outdoors or exerting themselves.

1.2.2.1 Athletes

Sports medicine and sports administration personnel are highly concerned with sporting participants' heat stress arising from vigorous exercise and the thermal environment because of the perceived risk of heat casualties (Brotherhood, 2008). Exertional heat stroke remains one of the leading causes of sudden death during sport (Casa et al., 2015). During training and competition, an athlete's metabolic heat production provokes significant physiological strain on the human body. Heat production during exercise is $15 - 18$ times greater than at rest and can raise T_c by 1°C every 5 minutes if no thermoregulatory modifications are made (Nadel et al., 1977). When adverse environmental conditions are present, such as high T_a and relative humidity (RH), they add to this metabolic heat load and prevent the

adequate heat loss needed to avoid overheating (Brotherhood, 2008). A warmer future will only add physiological strain to an individual's thermoregulation during physical activity. Maloney and Forbes (2011) found that for unacclimatized people in Australia, future outdoor physical activity will not be possible on $33 - 45$ days per year, compared to $4 - 6$ days per year at present.

In a prestigious sporting event such as the Summer Olympics or Summer Pan American Games, where milliseconds and millimeters often determine an athletes rank, the thermal environment and can be an important factor in affecting athlete performance. Therefore, many sports organizations frequently use heat stress metrics, such as the wet-bulb globe thermometer (WBGT) index, to monitor the risk of HR illness and to set environmental thresholds for training and competition (Casa et al., 2015; Larsen et al., 2007). Casa et al. (2015) recommend that public health officials establish on-site emergency response plans for their venues and athletes based on the environmental conditions of the site, the specific sport, and individual considerations to maximize athlete safety and performance. Many other indices have been developed for use in outdoor sporting events (see Epstein and Moran et al., 2006), however the WBGT index is the most well-known and used metric.

1.2.2.2 Mass Gathering Attendees

Mass gatherings are generally defined as a large number of people (ranging from 1,000 to $>$ 25,000) at a specific location, for a specific purpose, for a defined time frame (Perron et al., 2005). Attendees of mass gatherings face unique health risks because these events create challenging environments for EMS responses. High crowd density often limits attendee access to air flow, shade, and water, and the thermal insulation of surrounding bodies and metabolic heat generation adds to the

heat load already induced by the thermal environment (Helbing and Johansson, 2013). Steffen et al. (2012) found that HR illnesses are one of the leading causes of mortality at mass gatherings, with event type and weather commonly being the variables that best predict medical usage rates (Milsten et al., 2002; Milsten et al., 2004).

Patient information collected at three types of mass gatherings revealed that medical cases occurred more frequently at sporting events (Milsten et al., 2004). At large-scale sporting events, such as the 1996 Summer Olympic games in Atlanta Georgia, Wetterhall et al. (1998) determined that spectators and volunteers accounted for the vast majority of EMS visits for HR illness, while injury EMS visits were more common among athletes. This result makes sense as large-scale sporting events often attract spectators and volunteers from around the world who, as non-residents, are often poorly acclimatized to the local environmental conditions (Matzarakis and Frohlich, 2014). Contrarily, athletes often participate in heat acclimation training well in advance of afar competitions to prepare for competing in local weather conditions (Casa et al., 2015; Larsen et al., 2007).

1.2.2.3 Sports Tourists

Populations living in different climates have different susceptibilities (Jendritzky and Tinz, 2009), meaning that travel to new locations for sports-entertainment may result in health problems for non-natives (e.g. caused by heat stress) (Matzarakis, 2006). In assessing the thermal satisfaction levels of local residents and tourists at ten luxury hotels on the tropical island of Hainan, China, Lu et al. (2016) found that tourists were significantly more sensitive to the wind speed (V_w) and T_a considering the V_w compensation. Similarly, Lin and Matzarakis (2011) found only the northern-most regions of Taiwan and Eastern China to be

perceived as comfortable in the summer based on tourist thermal perceptions and thermal comfort (TC), defined as 'that condition of mind which expresses satisfaction with the thermal environment' (Fanger, 1972), classifications. As the interface between climate and tourism is multifaceted and complex (Scott and Lemieux, 2010), these results indicate that there will be thermal discomfort among attendees, with a higher likelihood of unacclimatized individuals experiencing heat stress if correct precautions are not taken. In fact, it has been the experience of medical personnel over multiple seasons of working at a large sports facility that the number of patients seen during a game correlates closely with game-time heat and humidity (Perron et al., 2004).

1.2.3 Emergency Medical Service Response Data

The vast majority of heat and human health research has focused on analyzing mortality data, thus causing a lack of information concerning the associations between heat and non-fatal illnesses (Dolney and Sheridan, 2006; McGeehin and Mirabelli, 2001). Dolney and Sheridan (2006) explain that this issue is largely because adequate and high quality morbidity data are often difficult to obtain. In recent years, however, worldwide epidemiological studies investigating heat and morbidity relationships through the use of EMS ambulance dispatches have begun to emerge (Graham et al., 2016; Cheng et al., 2016; Alessandrini et al., 2011, Ng et al., 2014).

Results from these studies, especially those focusing on a finer spatial scale, provide additional insight into neighborhood or individual vulnerability to extreme heat by identifying locations and times when a population may be at a greater risk of exposure to heat stress. Using EMS, land cover, and environmental information, Graham et al. (2016) discovered that even a marginal increase in the tree canopy

cover could reduce HR ambulance calls by approximately 80%. Further, Cheng et al. (2016) and Alessandrini et al. (2011) found that the percent change in the number of ambulance dispatches increased with every 1°C raise in temperature in Huainan, China and Emilia-Romagna, Italy, respectively.

There are several advantages to using EMS ambulance dispatch data to monitor HR illness, including the electronic availability of data on a near-real time basis and record of the location and time at which the patient actually became ill (Bassil et al., 2009). Because of HIPPA protection and ethical research practices, other health databases often record the patient's residential address, which results in coarser health information to use in weather-heath analysis; however, using EMS data, as in the current study, provides the exact time and location of when a HR issue occurred.

Also, a commonality among the current literature is that the weather data used to analyze the 'heat' portion of the heat-morbidity relationship in cities is obtained from either a single weather station (usually located at the airport) (Hartz et al., 2013) or the averaged values of scattered weather stations (Graham et al., 2016; Niu et al., 2016). As EMS response calls for HR illness are vastly spread throughout the city and intra-urban heating varies, using such weather data is likely misclassifying the exposure of individuals to their surrounding environmental conditions at the time the call was made. Therefore, the current study utilizes the unique combination of fine-scale mesonet weather data and EMS ambulance dispatch data to assess HR illnesses correlated with specific environmental conditions.

1.2.4 Urban Heat-Health Analysis at Varying Scales

The temporal and spatial variability in outdoor spaces is highly complex (Kenny et al., 2009a) and is largely pronounced within the built environment. This complexity arises at small scales from several physical features such as ambient

weather, urban design, air pollution, and the thermal properties of building and ground materials (Yaghoobian et al., 2010). The resulting thermal environment therefore can have a compelling effect (both negative and positive) on the health of its residents. Cities are mainly composed of artifical building materials that absorb and retain heat from daytime solar radiation fluxes. Within urban areas, however, locations exist that contain natural surfaces (vegetation, water, etc.) and shade that are associated with significant reductions in summer temperatures and improvements in TC (Vanos et al., 2016; Giannakis et al., 2016; Perini and Magliocco, 2014; Vanos et al., 2012c). This occurs because the albedo and water concentration of green spaces and hard artifical surfaces differ drastically due to evapotranspiration phenomena and the efficiency of plants in regulating both incident and reflected direct solar radiation (Salata et al., 2015). For this reason, Gill et al. (2007) insist that numerous finer-scale heat (and cool) islands can be identified within a larger city-wide UHI, dispersed in between the built environment and green or blue infrastructure (Gehrels et al, 2016).

Yet urban heat-health research regularly operates at coarse scales and uses scattered environment observations, while these urban features generally impact human health at small scales (Kuras et al., 2015). This coarser scale has resulted in a deficiency of spatially congruent evidence linking together urban form and human TC at the human scale (Solis et al., 2016). Since variations in urban characteristics can make one area of the city much warmer and less thermally comfortable than another (or vice versa), determining the degree of correlation between the weather in a single area of the city (exposure) and the number of HR illnesses (response) is important for mitigating negative effects on human health during extreme heat events.

1.3 The Impact of the Physical Environment on Heat Related Morbidity and Mortality

Empirically-based public health studies demonstrate that the monthly distribution of EMS ambulance dispatches due to HR illnesses peaks in the summer, with the majority of the elevated dispatch days having either maximum temperatures (T_{max}) considerably higher than normal or a T_a rise between neighboring days (Golden et al., 2008; Cheng et al., 2016). If high T_a is sustained during the overnight hours, T_a-associated mortality tends to increase (Kalkstein and Davis, 1989), indicating that T_{min} is an additional important parameter in the relationship between weather and health, as hot nights reduce the ability of the human body to recover from high daily T_{max}, particularly for those without air conditioning.

Although studies of HR morbidity and mortality have focused primarily on T_a, human TC is also affected by microclimatic variations in solar and terrestrial radiation, RH, and V_w (Brown et al., 2015; Erell et al., 2012). The mean radiant temperature (T_{mrt}) — the combination of all short and longwave radiant fluxes (Thorsson et al., 2007) — is a significant variable to consider in outdoor TC research because the radiation absorbed by a human (R_{abs}) is often the largest contributor to human heat gain and thermal discomfort in warm conditions (Johansson et al., 2014; Kantor et al., 2014; Taleghani et al., 2015; Kenny et al., 2008).

Additionally, Zhang et al. (2014) found that absolute humidity was frequently selected as one of the most important variables for all-cause mortality across multiple United States cities and V_w has been shown to be significantly correlated with human thermal satisfaction levels (Lu et al., 2016). Each study has subsequently recommended that both humidity and V_w be included in future heat-health studies, respectively. Studies have also expressed the need for further

research into determining the importance of specific weather parameters on the relationship between weather and health (McGeehin and Mirabelli, 2001). Doing so will improve our understanding of the heat-health relationship and aid in preventative procedures as key parameters' health-harmful thresholds are identified.

1.3.1 Heat Stress Metrics

Various countries now use univariate, bivariate, and multivariate heat stress metrics to help identify episodes of hot weather that are detrimental to human health (Smoyer-Tomic et al., 2001), which have been developed for a range of applications, from heat warnings to exertional heat illness guidelines. Each heat stress metric outputs a single value that represents scale-based neutral-to-dangerous conditions and can be split into one of three metric categories: empirical, direct, and rational (McGregor and Vanos, in review).

1.3.1.1 Direct Heat Stress Metrics

Direct heat stress metrics use only measurements of weather conditions to infer the thermal environment experienced by an individual (McGregor and Vanos, in review). The most common direct metrics used in heat-health literature are the heat index (HI), apparent temperature (AT), humidex, and WBGT index. Perron et al. (2004) indicate a strong positive correlation between the HI and the number of patients cared for during a sporting event, where linear models predict that for every 10-degree increase in the HI, three more patients per 10,000 people will require medical attention. Similarly, statistical analysis completed by Hartz et al. (2013) showed that of the five heat stress metrics assessed in Phoenix and Chicago, daily maximum AT had the strongest relationship with HR illness. Since the number of high heat stress days and nights (magnitude dependent on heat stress metric) during

summer is projected to increase in Toronto by the mid-21st century (Smoyer-Tomic and Rainham, 2001; Oleson et al., 2013), increased patient volume and deaths should be expected as well. The most serious limitation in using direct heat stress metrics is that they do not take into account physiological parameters, such as an individual's activity level, clothing, etc., which can introduce large under-estimation errors into any predictions of human health outcomes (Budd, 2008).

1.3.1.2 Rational Heat Stress Metrics

Rational heat stress metrics are complex mathematical models that combine aspects of both empirical and direct metrics to account for both the environmental and physiological variables that impact an individual's health (McGregor and Vanos, in review). The most common rational metrics used in heat-health literature are human energy budget (EB) models, such as the universal thermal comfort index (UTCI) (Jendritzky et al., 2012), the physiologically equivalent temperature (PET) (Hoppe, 1999), and the comfort formula (COMFA) outdoor EB model (Brown and Gillespie, 1986). The COMFA EB model has been used extensively in North America to assess the human TC during sedentary and physical activity at different conditioning levels (Kenny et al., 2009a,b; Vanos et al., 2012a,b,c). A significant positive correlation was found by Kenny et al. (2009a) between participant actual thermal sensation votes and predicted EBs. Vanos et al. (2012c) likewise observed that HR emergency response calls were significantly dependent on the COMFA EB estimations of human TC within-city station data, thus suggesting that outdoor EB modeling has potential to be used as a guide for human heat stress prediction in addition to urban design (Brown et al., 2015).

Many heat-health studies have examined the ability of direct and rational metrics to predict health outcomes; however, there is no single existing heat metric

that is agreed upon to best predict human health response to heat stress because relationships vary by location, time of year, and population (Hajat et al., 2010). Correspondingly, the current study will investigate the ability of a combination of direct and rational heat stress metrics to predict HR EMS ambulance dispatches during the summertime in Toronto.

1.4 Study Goals and Objectives

Much of the prior literature examine heat-health relationships at scales that are large (such as city-wide). Relatively less attention has been paid to highlighting direct and indirect heat-health processes at finer scales, using ambient temperature, although many studies have used remotely-sensed surface temperatures to infer hot spots (Jenerette et al., 2016). Depending on their scale, some studies may therefore over- or under-estimate the potential heat-health response at specific environmental conditions (Tamerius et al., 2007). Currently, no study exists that evaluates the relationship between heat and human morbidity by utilizing the unique combination of fine-scale within-city meteorological mesonet stations and EMS ambulance response call data during a large-scale event. This is of great concern due to the vast differences in land characteristics across urban landscapes that control the thermal environment and the consequent potential heat stress experienced by a higher population of people in the given urban environment.

Accordingly, the goal of this study is to investigate the relationship between various heat stress metrics with heat illness in Toronto, Canada during the summer of 2015 during which the Pan and Parapan American Games took place. To do so, the following objectives will be accomplished:

1. Utilizing 53 mesonet stations, create spatial maps of the Greater Toronto Area (GTA) based on multiple heat metrics to demonstrate a) variations by metric

and b) where heat exposures are escalated.

2. Determine which heat metric has the strongest relationship with heat-related emergency response calls within the city limits of Toronto using statistical regression modeling and three spatial exposure proxies.

3. Perform athlete/spectator human energy budget case studies during Games sporting events at venues of escalated risk of exposure.

CHAPTER 2
METHODS

2.1 Study Site

Toronto, Canada [43.7182°N, 79.3774°W], the capital of the province of Ontario, is a dynamic metropolis along Lake Ontario's northwestern shore (see Figure 2.1). It is the largest city in Canada, hosting over six million residents within the greater area. The city experiences a semi-continental climate, with a generally warm, humid summer and a cold, dry winter, modified by its location on the shores of Lake Ontario (Peel et al., 2007). The three hottest months are June, July, and August, with average daily high temperatures of 23.8°C, 26.6°C, and 25.5°C respectively (Table 2.1). Located in the warmest climatic zone in Canada, Toronto has experienced above average T_{max} in five of the seven summers between 2010 and 2016 (Environment Canada, 2016), is subjected to UHI effects (Rinner and Hussain, 2011; Wang et al., 2016), and is predicted to have doubled HR mortality by 2050 and tripled HR mortality by 2080 (Penney, 2008). A maturing public-health risk to heat is predicted by Lemmen et al. (2008), proclaiming that Toronto will most likely experience more intense and frequent extreme heat events in the future. For this reason, heat-health alert systems have become the norm in cities of dense occupation. This tactic was used in Toronto for the 2015 summer season, in attempt to minimize human HR morbidity when an influx of athletes and public spectators occurred as a result of the Games.

2.2 Data Collection

This study incorporated two main datasets: a mesonet monitoring network meteorological dataset and an EMS ambulance response call dataset.

Table 2.1: Montly average climate data for Toronto, Canada (from 1981-2010).[1]

Month	High Temperature	Low Temperature
January	−0.7°C	−6.7°C
February	0.4°C	−5.6°C
March	4.7°C	−1.9°C
April	11.5°C	4.1°C
May	18.4°C	9.9°C
June	23.8°C	14.9°C
July	26.6°C	18.0°C
August	25.5°C	17.4°C
September	21.0°C	13.4°C
October	14°C	7.4°C
November	7.5°C	2.3°C
December	2.1°C	−3.1°C

[1] Information retrieved from Environment Canada (2017).

2.2.1 Environment Canada Mesonet Monitoring Network

In preparation for the Games, the Meteorological Service of Canada (MSC), a unit within Environment Canada, collaborated with Health Canada and Toronto Public Health to design a health and weather package that would encompass monitoring and prediction products on the themes of air quality, heat, and radiation in Toronto during the summer of 2015. This package promoted the installation of a mesonet monitoring network, consisting of 53 weather stations that were dispersed throughout the Games area, as displayed in the GIS map of Toronto in Figure 2.1. Of those 53 stations, 10 are permanent stations and 43 are compact stations that were temporarily installed. Figure 2.2 shows the general design of the compact weather stations. Each station was equipped with a black globe temperature sensor (Campbell Scientific, Inc.) to record globe temperature (°C), and either a Vaisala WXT520, Lufft WS601, or Lufft WS600 weather transmitter to record V_w (m/s) and wind direction, T_a (°C), dewpoint temperature (°C), wet-bulb temperature (°C), and RH (%). Instrument height for all stations was 2.5m above their

respective surface.

A list of each station's name, local climate zone (LCZ), latitude, and longitude can be found in Appendix A. All station LCZs were classified based on categories from Stewart and Oke (2012; Table 2). Considering the surrounding environment (up to 250m), the LCZ of a station was determined post-site selection process, using notes and photos taken by the MSC while on-site and Google Earth. Any LCZ or height differences among the stations were accounted for upon installation. The compact stations were primarily installed in 2014 and decommissioned in Fall 2015, and were operational from May 2015 through September 2015. However, this study focuses only on the data collected during July and August; the months during which the Games took place. During the Games, a mobile application relaying real-time weather information (provided by Environment Canada) from each station was available for public use to warn users of potential adverse weather conditions at their location on event days.

Data were collected at 1-min intervals using either a CR-1000 or CR-3000 Campbell Scientific datalogger. Any missing data was recorded as missing and was not included in the analysis. 48 of the stations had $\leq 1.1\%$ of data missing, 3 stations had $< 8\%$ of data missing, and 2 stations had $< 18\%$ of data missing (6156131 and 6136305). Neither of the 2 stations with $> 8\%$ of their data missing were used in the finer-scale heat metric and EMS ambulance response call analysis, yet were included in the heat metric maps. The meteorological variables used within this study are calculated as averages over the past 1 hr. The maximum and minimum value over the past 1 hr was additionally extracted for T_a. These data are representative of the meteorological environment around each station in which outdoor human activity took place. As previously mentioned, such fine-scale surveillance has the potential to initiate an early and targeted public health

response and mitigate the harmful health effects of extreme temperature.

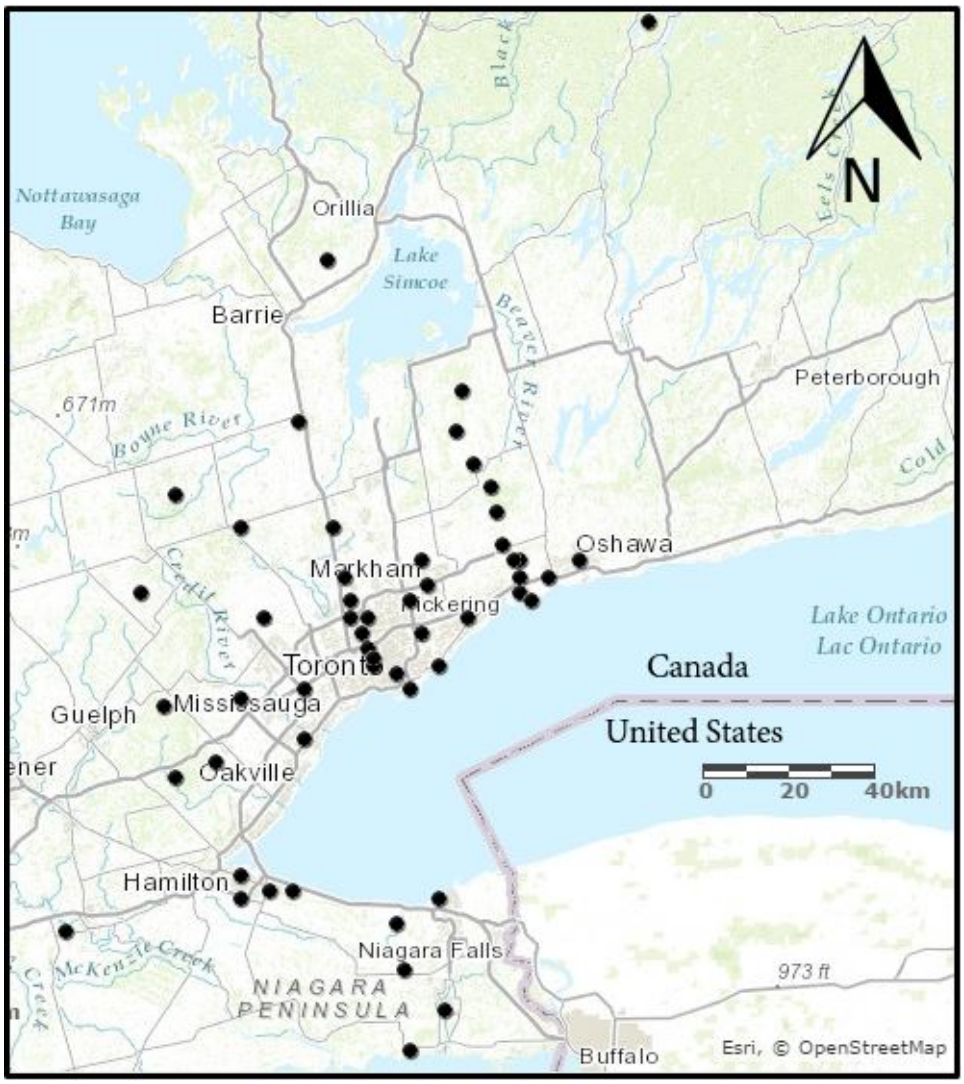

Figure 2.1. Mesonet monitoring network stations (black circles) dispersed across the Games area. The stations are generally located near the Games venues.

2.2.2 Heat Stress Metrics

From the meteorological variables collected by the mesonet monitoring network, three heat metrics were calculated: the humidex, the WBGT index, and the COMFA human EB.

Figure 2.2. General structure of one of the 43 temporarily installed compact mesonet stations used to monitor environmental conditions during the Games. Source: Environment Canada.

2.2.2.1 Humidex

Canadian meteorologists use the humidex to interpret a perceived temperature, or one that the average human body would feel, given the combination of the T_a and RH of the air. The humidex is an empirically-derived method of quantifying human discomfort due to excessive heat and humidity. The current equation for computing the humidex, in °C, developed in 1979 by Masterton and Richardson of Canada's Environment Service, is as follows:

$$\text{Humidex} = T_a + 0.5555\left[6.11e^{5417.7530\left(\frac{1}{273.16}-\frac{1}{T_{dew}}\right)} - 10\right] \tag{2.1}$$

where T_a is the air temperature in °C and T_{dew} is the dewpoint temperature in K. Environment Canada uses a humidex assessment scale to alert the public of thermally uncomfortable conditions based on the degree of comfort associated with the scale ranges; $20 - 29$°C 'Little Discomfort', $30 - 39$°C 'Some Discomfort', $40 - 45$°C 'Great Discomfort; Avoid Exertion', above 45°C 'Dangerous; Heat Stroke Possible' (Blazejczyk et al., 2012, Table 2).

2.2.2.2 Wet-Bulb Globe Temperature (WBGT) Index

The WBGT index, originally created in the early 1950s to limit serious heat illness outbreaks in the United States Armed Services training camps, is commonly used in heat stress research (Budd, 2008). In addition to T_a and humidity, the WBGT index incorporates the effects of solar radiation and V_w: two vital ingredients for assessing human heat stress in adverse outdoor microclimates. The index is a weighted average of the natural wet-bulb temperature (T_w) in °C, dry-bulb air temperature (T_a) in °C, and globe temperature (T_g) in °C, calculated as:

$$\text{WBGT} = 0.7T_w + 0.2T_g + 0.1T_a. \tag{2.2}$$

Today the WBGT index remains a convenient and comprehensive index of heat stress used to monitor environmental conditions during manual labor and exercise in direct sunlight. Based on the magnitude of the index output and the type of physical activity being performed in the heat (e.g. military training, athletics programs, work), specific guidelines have been established for activity modifications to avoid experiencing heat stress (e.g. rest breaks, water consumption, limited uniform attire) (Armstrong, 2007). Table 2.2 provides an example of WBGT index threshold guidelines for athletic workouts and/or competition.

Table 2.2. WBGT levels for modification or cancellation of workouts or athletic competition for healthy adults (adapted from Armstrong et al., 2007).[d]

WBGT °C	**Nonacclimatized, Unfit, High-Risk Individuals**[a]	**Acclimatized, Fit, Low-Risk Individuals**[a,b]
≤ 10	Normal activity	Normal activity
10.1 - 18.3	Normal activity	Normal activity
18.4 - 22.2	Increase the rest:work ratio. Monitor fluid intake.	Normal activity
22.3 - 25.6	Increase the rest:work ratio and decrease total duration of activity.	Normal activity. Monitor fluid intake.
25.7 - 27.8	Increase the rest:work ratio; decrease intensity and total duration of activity.	Normal activity. Monitor fluid intake.
27.9 - 30.0	Increase the rest:work ratio; decrease intensity and total duration of activity. Limit intense exercise. Watch at-risk individuals carefully.	Plan intense or prolonged exercise with discretion[d]; watch at-risk individuals carefully.
30.1 - 32.2	Cancel or stop practice and competition.	Limit intense exercise[d] and total daily exposure to heat and humidity; watch for early signs and symptoms.
< 32.3	Cancel exercise.	Cancel exercise uncompensable heat stress[c] exists for all athletes[d].

[a] while wearing shorts, T-shirt, socks and sneakers.
[b] acclimatized to training in the heat (for at least 3 weeks).
[c] internal heat production exceeds heat loss and core body temperature rises continuously, without a plateau.
[d] Differences of local climate and individual heat acclimatization status may allow activity at higher levels than outlined in the table, but athletes and coaches should consult with sports medicine staff and should be cautious when exceeding these limits.

The main limitation of the WBGT index is that it does not adequately account for the added heat stress humans experience when the evaporation of sweat is restricted by high humidity, low air movement, or clothing (Budd, 2008). However, adapted (lower) thresholds have been created in order to account for additional clothing or early season heat exposure (Armstrong, 2007). The Canadian Centre for Occupational Health and Safety (CCOHS), in particular, has comprised a list of adjusted threshold limit values for the WBGT index based on the type of work clothing being worn (Government of Canada, 2017).

2.2.2.3 Comfort Formula (COMFA) Human Energy Budget

The COMFA outdoor EB model is a metric designed to assess the heat stress of humans performing physical activity. Many studies have both tested and incorporated revisions into the model to ensure maximum agreement between tested subjects environment-based TC and the budget output (Brown and Gillespie 1986; Kenny et al. 2009a,b; Vanos et al. 2012a,b,c). It requires meteorological inputs (T_a, R_{abs}, RH, and V_w) and physiological inputs (metabolic activity, M_{act}, and activity velocity, V_a) to produce a human EB in Wm^{-2}, calculated as:

$$\mathrm{EB} = M + R_{abs} - E - C - L_{emit} \tag{2.3}$$

where M is the metabolic heat generated by a human, R_{abs} is the radiation absorbed by a human, E and C are the total evaporative and convective heat losses from a human, respectively, and L_{emit} is longwave radiation emitted from a human. All fluxes are in Wm^{-2}. The subjective interpretation of the model output values for sedentary individuals is displayed in Table 2.3 (Brown and Gillespie, 1986; Kenny et al., 2009a). Full COMFA EB model explanations and equations can be found in Brown and Gillepsie (1986) and Kenny et al. (2008; 2009a,b). The EB and the associated flux components (EB streams) are calculated using the most recent version of the COMFA EB model (Vanos et al., 2012c; Kenny et al., 2009b).

In the analysis for objectives 1 and 2, a constant M_{act} of 87.15 Wm^{-2} was used to represent a M_{act} of a standing, slowly walking human performing little activity, replicating that of a tourist/event spectator. As humans often base their clothing choices on the weather, intrinsic clothing insulation estimations were based on

Table 2.3. Subjective interpretation of the COMFA EB model output values for a sedentary individual (sitting or standing) (Brown and Gillespie, 1986).

Subjective Interpretation	Model Output (Wm^{-2})
'Cold'(−3)	≤−201
'Cool'(−2)	−200 to −121
'Slightly Cool'(−1)	−120 to −51
'Neutral'(0)	−50 to +50
'Slightly Warm'(+1)	+51 to +120
'Warm'(+2)	+121 to +200
'Hot'(+3)	≥+201

ambient T_a, as follows:

$$I_{cl} = 1.372 - 0.01866T_a - 0.0004849T_a^2 - 0.000009333 - T_a^3 \tag{2.4}$$

where T_a is air temperature in °C, and I_{cl} is clothing insulation in units of clo, which is an arbitrary unit (1 clo = 186.6 sm^{-1} = 0.1555 m^2 $°C^{-1}$ W^{-1}) (UTCI, 2010; Havenith et al., 2012; Psikuta et al., 2012). Because the clothing of tourists/spectators was unknown, this can accurately estimate the attire of a human whom TC is being calculated for.

Similarly, for the given study, the R_{abs} is determined by calculating the T_{mrt} using the globe thermometer, and converting the temperature into an R_{abs} energy flux in Wm^{-2}. Using the globe temperature, we first calculate the T_{mrt} (Equation 2.5) (Johansson et al., 2014) for input into Equation 2.6 to determine R_{abs}.

$$T_{mrt} = \left[(T_g + 273.15)^4 + \frac{(1.335 \times 10^8)V_w^{0.71}}{E(D^{0.4})}(T_g - T_a)\right]^{1/4} - 273.15 \tag{2.5}$$

where T_a is air temperature in °C, T_g is globe temperature in °C, V_w is wind speed

in ms^{-1}, E is the globe emissivity (0.95), D is the globe diameter (0.150m).

$$R_{abs} = \sigma(T_{mrt} + 273.15)^4 \tag{2.6}$$

where σ is the stefan-boltzmann constant (5.67×10^{-8} $Wm^{-2}K^{-4}$) (Johansson et al., 2014). However, T_g values are based on a black spherical human with an albedo near 0, yet humans are mainly cylindrical-shaped with an average albedo of about 0.37 (Brown and Gillespie, 1986; Montieth and Unsworth, 1990); therefore, the R_{abs} values calculated from the black globe in Equation 2.6 would over-predict the actual absorbed radiation experienced by a human, mainly due to the black matte color. Hence, a correction factor was applied to each R_{abs} value to account for color differences and geometric differences between a cylinder and globe at every solar angle, as in Grundstein et al. (2017).

2.2.3 EMS Response Calls

The main EMS dataset for the study dates was obtained from the Toronto Emergency Medical Services (TEMS) medical dispatch database under a data sharing and confidentiality agreement. The study also received ethics approval from Texas Tech University. The dataset included all 911 emergency medical dispatch calls, both HR and non-heat-related (NHR), to which TEMS responded within the Toronto city limits (see Figure 2.3). The following variables were extracted for each call: response date, patient gender, patient age, Medical Priority Dispatch System (MPDS) determinant code, and latitude and longitude coordinates of the pick-up location. The MPDS determinant code reports the issue and the severity of the call (Graham et al., 2016). A full explanation on how MPDS information is assigned to a call is provided in Bassil et al. (2009).

Bassil et al. (2008) found that the MPDS determinant code 'Heat/Cold

Exposure' corresponds well with T_a in Toronto, yet the use of this determinant code by TEMS is limited and consequently potentially misleading in regard to the full impact of heat on morbidity. The current study therefore used a broader subset of MPDS codes specified by Luber and McGeehin (2008) and utilized in more recent EMS heat-health studies in Toronto (Vanos et al., 2012a; Graham et al., 2016) and defined HR EMS calls as those that included the following conditions: Breathing Problems; Cardiac or Respiratory Arrest/Death; Chest Pain; Headache; Heart Problems; Heat/Cold Exposure; Sick Person; Stroke/Cerebrovascular Accident; and Unconscious/Fainting. Only 'Heat Exposure' calls were used from the 'Heat/Cold Exposure' MPDS determinant code category.

2.2.3.1 Spatial Distribution of EMS Response Calls

Daily total HR and NHR EMS calls were calculated for each 24-hr period of interest both city-wide and by station subdivision using nearest-neighbor analysis. Nearest-neighbor analysis is useful in analyzing the spatial relationship between features by finding the point (in this case, an EMS call) in a given set that is nearest to a given point (in this case, a weather station). Only the 14 stations that were either inside or outlining the Toronto city limits (see Figure 2.3) were used for this analysis. Table 2.4 shows the total number of HR and NHR EMS calls for the entire city and for each station for July and August 2015.

2.2.3.2 Spatial Variations

Due to the influx of over 7,000 athletes and an unknown number of volunteers and spectators in Toronto during the Games months attending numerous venues at varying times, it was not possible to use the standard census of population within the city to account for spatial and temporal differences in HR EMS calls. Instead,

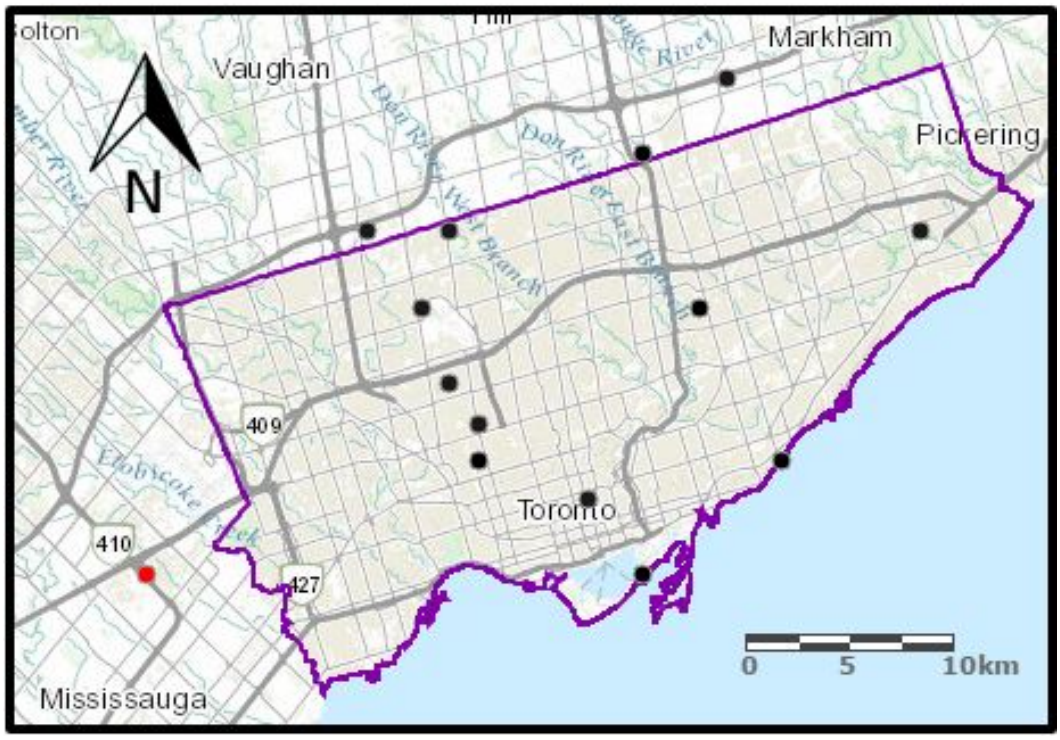

Figure 2.3. The 14 mesonet monitoring network stations (black circles) dispersed within or near the City of Toronto limits (outlined in purple). The weather station closest to the airport, used for the 'airport proxy', is displayed in red to the left of the city limits.

NHR EMS calls were used as a proxy for population counts. The ratio of the average HR and NHR EMS calls made during the Games period versus the non-Games period was assessed for both the individual stations and the stations combined. Minimal differences were found in the ratios; 0.71 for the Games period and 0.75 for the non-Games period for the full city. Therefore it was determined that no adjustment to HR EMS calls needed to be made during the Games period to account for population increases.

Table 2.4. Total number of heat-related and non-heat-related EMS ambulance response calls by station for July and August 2015.

STATION NUMBER	HR	NHR
City	11773	15878
6156164	367	543
6156170	542	639
6156161	504	613
6156168	921	1224
6156177	503	561
6156157	1712	2227
6156175	3021	4000
6156171	236	393
6156165	368	466
6156136	1364	1871
6156172	881	1198
6156180	114	201
6156179	851	1215
6156183	389	727

2.3 Greater Toronto Area Heat Metric Maps

For each of the 53 mesonet weather stations, the daily maximum value of each of the calculated heat metrics, including T_{max}, was extracted for every day of July and August 2015. The daily maximum values for each heat metric were then averaged over the 62-day analysis period to create a seasonal summer average for each station. Graduated symbol classes in ArcGIS were used to plot the station-specific seasonal summer averages for each metric, respectively, to show variations by metric and where human exposure to HR illness is escalated.

2.4 Calculations of Relationships between Heat Metrics and EMS Response Calls

As EMS data were only available for the City of Toronto limits (see Figure 2.3), the 14 stations within the city were used to complete statistical regression modeling

to relate HR EMS ambulance response call data to the calculated heat metrics, including T_{max} and T_{min}. Three spatial exposure proxies were used for this analysis: 1) daily data used from only a single-station to represent the meteorological environment of the city per day, similar to how previous heat-health studies use airport weather station data (Hartz et al., 2013; Hondula et al., 2012) (herein denoted as the airport proxy), 2) daily data averaged across the 14 stations to represent the meteorological environment of the city per day (Graham et al., 2016) (averaged-city proxy), and 3) station-specific local data combined across the 14 within-city stations rather than by day (station-specific proxy). This is the first study that we know of to employ the station-specific exposure proxy.

For each spatial exposure proxy, an ordinary least squares (OLS) regression was applied and the 95% confidence intervals (CIs), variance (R^2 value), significance of the correlation (p-value), and the slope of the regression were calculated for comparison. The slope of the linear regression line represents the relative change in number of HR EMS calls per 1°C or 1 Wm^{-2}. A p-value of 0.05 was chosen to indicate that a heat stress metric is significantly correlated with the HR EMS calls. All dependent data were tested for linearity, collinearity, and normality, and were found to have a linear relationship with the independent variable of HR EMS calls. Normality testing was completed using the Shapiro-Wilks test of normality.

As HR EMS calls made during the early hours of the morning are generally resultant of the previous day's environmental conditions, a brief time frame shift analysis was constructed to determine the extent to which proceeding morning calls were related to the previous day's weather. We tested no time shift and the 5:00am − 8:00am hour time shifts in hourly intervals. Results from this time frame shift analysis are shown in Table 2.5. A shift to 5:00am showed the strongest relationship and therefore, for all analysis in objective 2, all EMS calls made between 12:00am

and 5:00am local standard time (LST) were added to the preceding day's total HR EMS call count. For example, any HR EMS calls made between the hours of 12:00am and 5:00am on July 2nd were added to the total number of HR EMS calls recorded between 5:00am and midnight on July 1st. The coinciding NHR EMS calls were also assigned to the preceding day's total NHR EMS call count to keep the respective number of HR EMS calls per population counts consistent.

2.4.1 Airport Proxy

The daily value of each heat stress metric recorded by the mesonet weather station closest to the Toronto Pearson International Airport (Hershey Centre, shown on Figure 2.3) was plotted against the daily city-wide total number of HR EMS calls per 100,000 people. The total number of HR EMS calls made at a given heat metric value was determined by taking the ratio of total HR-to-NHR calls and scaling it to a population of 100,000 people. To scale the HR-to-NHR EMS call ratio to a population estimate, the total number of NHR EMS calls over the entire study period (15,878 calls) was divided by the number of days in the study period (62 days) and divided by the population of Toronto City (2.7 million) and multiplied by 100,000 to get the total HR-calls-per-100,000 people, as follows:

$$\text{Total HR EMS Calls per 100,000} = \frac{\text{HR Calls}}{\text{NHR Calls}} \times \frac{\text{Total NHR Calls}}{\text{62 Days}} \times \frac{\text{100,000}}{\text{City Population}}. \tag{2.7}$$

This ratio of per 100,000 people is commonly used in health literature to describe the relationships between a health issue and a population (Scutchfield and Keck, 2003). This method for determining the total number of HR EMS calls was applied to both the averaged-city and station-specific proxies as well. Applying this approach is important in order to compare the statistical results within and between

Table 2.5. Time frame EMS ambulance response call statistical analysis results for time shift correction.

0:00 LST	Airport		Averaged-City		Station-Specific	
	Slope	R^2	Slope	R^2	Slope	R^2
T_{max}	0.010	0.002	0.026	0.012	0.042	0.048
T_{min}	0.046	0.029	0.043	0.025	0.067	0.080
Humidex	0.012	0.007	0.020	0.015	0.024	0.024
WBGT	0.004	0.0003	0.039	0.018	0.034	0.018
COMFA	0.0008	0.0078	0.0030	0.0685	0.0028	0.0693
5:00 LST	Airport		Averaged-City		Station-Specific	
	Slope	R^2	Slope	R^2	Slope	R^2
T_{max}	0.020	0.008	0.029	0.016	0.042	0.044
T_{min}	0.047	0.031	0.056	0.039	0.066	0.081
Humidex	0.002	0.000	0.024	0.021	0.023	0.031
WBGT	0.001	0.000	0.025	0.009	0.036	0.019
COMFA	0.0020	0.0482	0.0034	0.0753	0.0033	0.1119
6:00 LST	Airport		Averaged-City		Station-Specific	
	Slope	R^2	Slope	R^2	Slope	R^2
T_{max}	0.025	0.012	0.033	0.020	0.046	0.053
T_{min}	0.042	0.024	0.051	0.031	0.063	0.067
Humidex	0.014	0.008	0.022	0.018	0.026	0.037
WBGT	-0.002	0.000	0.028	0.011	0.032	0.013
COMFA	0.0025	0.0668	0.0039	0.1084	0.0033	0.1065
7:00 LST	Airport		Averaged-City		Station-Specific	
	Slope	R^2	Slope	R^2	Slope	R^2
T_{max}	0.023	0.011	0.036	0.023	0.043	0.042
T_{min}	0.037	0.018	0.040	0.019	0.058	0.051
Humidex	0.016	0.011	0.024	0.020	0.024	0.033
WBGT	0.007	0.001	0.030	0.018	0.031	0.012
COMFA	0.0023	0.0573	0.0037	0.0961	0.0032	0.1099
8:00 LST	Airport		Averaged-City		Station-Specific	
	Slope	R^2	Slope	R^2	Slope	R^2
T_{max}	0.021	0.009	0.031	0.016	0.040	0.038
T_{min}	0.026	0.009	0.027	0.010	0.046	0.033
Humidex	0.009	0.003	0.021	0.015	0.016	0.019
WBGT	0.005	0.000	0.030	0.010	0.027	0.009
COMFA	0.0024	0.0619	0.0041	0.1082	0.0032	0.0975

each of the proxies with respect to their ability to predict HR EMS calls. The airport proxy represents the degree of correlation that can be expected when a single-station's weather data is used to represent the environmental conditions of all locations within a city.

2.4.2 Averaged-City Proxy

The daily value of each heat stress metric recorded by each individual station was averaged over the 14 stations to create a daily city-wide heat stress metric value. This value was then correlated to the daily city-wide HR EMS call total per 100,000 people. The averaged-city proxy represents the degree of correlation that can be expected when overall averaged weather data is used to represent the environmental conditions of all locations within a city, which is a method used within environmental health studies (Graham et al., 2016; Niu et al., 2016).

2.4.3 Station-Specific Proxy

Finally, the station-specific proxy sums the number of HR EMS calls made at a specific heat metric value (e.g., T_{max} of 30°C) across the 14 stations. For example, if each of the 14 stations recorded 10 HR EMS calls on the same day that they recorded a T_{max} of 30°C, the total number of HR EMS calls made at that specific heat metric value (30°C) would be 140. This final method better represents the local meteorological environment of the location at which an individual HR EMS call was made and provides a more robust estimate for statistical analysis. The total number of HR EMS calls made at each heat metric value were distributed among 62 evenly-weighted bins with approximately the same number of NHR EMS calls in each bin. This binning is important in order to perform an OLS regression for comparative purposes with the airport and averaged-city proxies. Within each bin,

the number of HR EMS calls correlated with each heat stress metric value were summed. The mean heat metric value of each bin was used in the OLS regression fitting process.

2.5 Athlete and Spectator Human Energy Budget Case Studies

Anecdotal evidence from Environment Canada, Hamilton Paramedic Service, and St. John Ambulance were received regarding excess spectator heat stress complaints and HR EMS response calls recorded at certain venues during the Games events. Events of interest included the men's bronze medal soccer match and women's gold medal soccer match on July 25th, and the men's gold medal soccer match on July 26th. These events occurred at the Hamilton Pan Am Soccer Stadium, henceforth referred to as 'Hamilton Soccer Stadium'.

Minutely weather data from the mesonet station placed at Hamilton Soccer Stadium (see Figure 2.4) were used for the meteorological inputs required by the COMFA EB model to calculate the EBs of the athletes and spectators in attendance at each of the events of interest. The R_{abs} experienced by athletes and spectators alike was calculated by Equation 2.6, where an α of 0.37 and an A_{eff} of 0.78 were used to represent the albedo of a human and the effective area of a standing human body that is exposed to radiation, respectively (Kenny et al., 2008). All physiological input values for the athletes and spectators are shown in Table 2.6.

For athletes, physiological inputs to the COMFA EB model were based on the activity of three main positions played in the sport of soccer; midfielder, defender, and goalie. In order to provide more accurate estimates of what a soccer player experiences in a given game (as opposed to using a constant metabolic intensity (MET) value of 8.0 METs using the compendium of physical activities (Ainsworth et al., 2011) and a 0 activity speed), data were applied from a competitive soccer

Figure 2.4. Hamilton Soccer Centre mesonet station used to monitor environmental conditions during the Games' soccer events. Source: Environment Canada.

game completed at Texas Tech University on a warm spring day, since no physiological data was available from the Games events. Using the MET value from Ainsworth et al. (2011) would result in highly inaccurate estimates by assuming a constant M_{act} for the entire game, which is unrealistic, as is the use of no V_a. Thus, although the data used here are not from the actual soccer games of interest mentioned above, they provide significantly improved estimates of the activity conditions experienced by a soccer player, as they are from a competitive, high level soccer game during warm conditions. To obtain these soccer player's M_{act} estimates, players wore Polar Team Pro heart rate sensors, which measured heart rate (bpm), V_a (ms^{-1}), acceleration (ms^{-2}), and distance (m) at 1-sec intervals, converted to 1-min averages to align with the weather station data. Analogous to the energy

expenditure estimation method used in Vanos et al. (in review) from Strath et al. (2000), inputs of age, resting heart rate, activity heart rate, and gender were used to estimate the energy expenditure of the players, which was output in METs (1 MET = 58.15 Wm^{-2}).

Spectator physiological inputs were modeled as a "very excited, emotional, and cheering" individual (MET = 3.0) (Ainsworth et al., 2011) (see Table 2.6). Athletic soccer clothing estimations were based on the standard configuration of a soccer uniform. The athletic clothing ensemble insulation estimation was determined by:

$$I_{cl} = 0.161 + 0.835 \sum I_{clu} \tag{2.8}$$

where I_{clu} is the effective thermal insulation of the individual garments making up the athlete clothing ensemble in clo (ISO, 2007 Eq. 11). From ISO (2007), the I_{clu} for the individual garments of a soccer uniform were briefs/panties (0.03 clo), shirt (0.07 clo), shorts (0.07 clo), knee-length thick socks (0.06 clo), and soft-soled athletic shoes (0.02 clo), respectively, resulting in an I_{cl} of 0.37 clo. Similarly, spectator clothing estimations were based on typical summertime attire, which includes underwear, a T-shirt, shorts, light socks, and sandals (0.33 clo) (ISO, 2007 Table A.1).

The EB experienced by spectators was determined by using the subjective interpretation shown in Table 2.3. Athletes, however, are prepared and more acclimatized, accepting, and expectant of uncomfortable conditions, with better conditioning resulting in better higher sweat rates and lower heart rates and T_c, allowing the body to more effectively cope with thermal stressors while performing physical activity (Casa et al., 2015). For this reason, the EB experienced by competing soccer athletes are based on a modified subjective interpretation of the

Table 2.6. Physiological inputs used for the spectator and athlete (soccer player) in the COMFA model.

Human	Input	Value
Spectator	M_{act}	166 Wm^{-2}
	V_a	0.2 ms^{-1}
	clo	0.33
	A_{eff}	0.78
	α	0.37
Athlete	M_{act}	varying
	V_a	varying
	clo	0.37
	A_{eff}	0.78
	α	0.37

original COMFA values developed for sedentary individuals based on Kenny et al. (2009b) and Harlan et al. (2006) shown in Table 2.7.

Table 2.7. Subjective interpretation of the COMFA EB model output values for athletes performing physical activity (Kenny et al., 2009b).

Subjective Interpretation	Model Output (Wm^{-2})
'Cold'(−2)	≤ -151
'Cool'(−1)	−150 to −20
'Neutral'(0)	−20 to +150
'Warm'(+1)	+151 to +250
'Hot'(+2)	$\geq +251$

CHAPTER 3

RESULTS

Based on the objectives, the main findings of this study demonstrate that overall: 1) all heat stress metrics indicate Hamilton, Ontario as an area of escalated heat exposure within the GTA, 2) generally weak relationships existed between HR calls and the heat metrics, yet the station-specific proxy showed the strongest relationships with HR EMS response calls, and 3) spectator and physically active athlete human EBs during the Games soccer events showed that the greatest heat stress was experienced during the women's gold medal match, aligning with R_{abs} and M_{act} values as the greatest contributors to the experienced heat stress.

3.1 Greater Toronto Area Heat Maps

The station-specific seasonal summer averages for each heat stress metric (T_{max}, humidex, WBGT index, and COMFA) are presented with size and color of circles in Figures 3.1 − 3.4. The numerical seasonal summer average values for each station for the four heat metrics can be found in Appendix B. The stations with the highest T_{max} values are concentrated near the cities of Toronto [43.7182°N, 79.3774°W] and Hamilton [43.2557°N, 79.8711°W] − two of the most built-up and populated urban areas within the GTA. The humidex is highest among the stations that are within close proximity to Lake Ontario and Lake Erie. A similar trend is observed by the WBGT index, which is also highly sensitive to the amount of moisture in the air (see Equation 2.2). It is evident that the area between Lake Erie and Lake Ontario creates a very humid environment as high humidex and WBGT index values are observed at stations located between the two lakes.

However, it is noticeable that the T_{max}, humidex, and WBGT index metrics'

values vary minimally among the stations, with ranges < 4°C. The COMFA metric has a much larger range of values given the unit of energy at Wm^{-2}, with the highest values demonstrating a more random distribution than the other heat metrics. This randomness is likely due to the COMFA model's dependence on multiple meteorological variables, meaning that location-specific wind and radiation − and hence localized atmospheric-convection − conditions are principal influentional factors, which are not factors in the other four metrics.

Much of the heat mapping results for objective 1 are devoted to detecting high-heat-exposure areas known as hot spots. Within the GTA, the city of Hamilton emerges as a hot spot across all of the heat metrics, with the Hamilton Soccer Center station ranking within the top 4% of the T_{max}, humidex, and WBGT index metric seasonal summer average values among all of the stations. Hamilton Soccer Center ranked within the top 30% of all COMFA seasonal summer average station values. A two-sample t-test also confirmed that Hamilton Soccer Center station was significantly different from the mean of all stations for the T_{max}, humidex, and WBGT index heat metrics. For these reasons, athlete and spectator EBs were modeled at three Games soccer events in late July at the Hamilton Soccer Stadium (Section 3.4) to assess the extent to which the weather conditions in Hamilton had an impact on human TC. More descriptive information will be presented in Section 3.4 regarding athlete and spectator EBs during a mass sporting event.

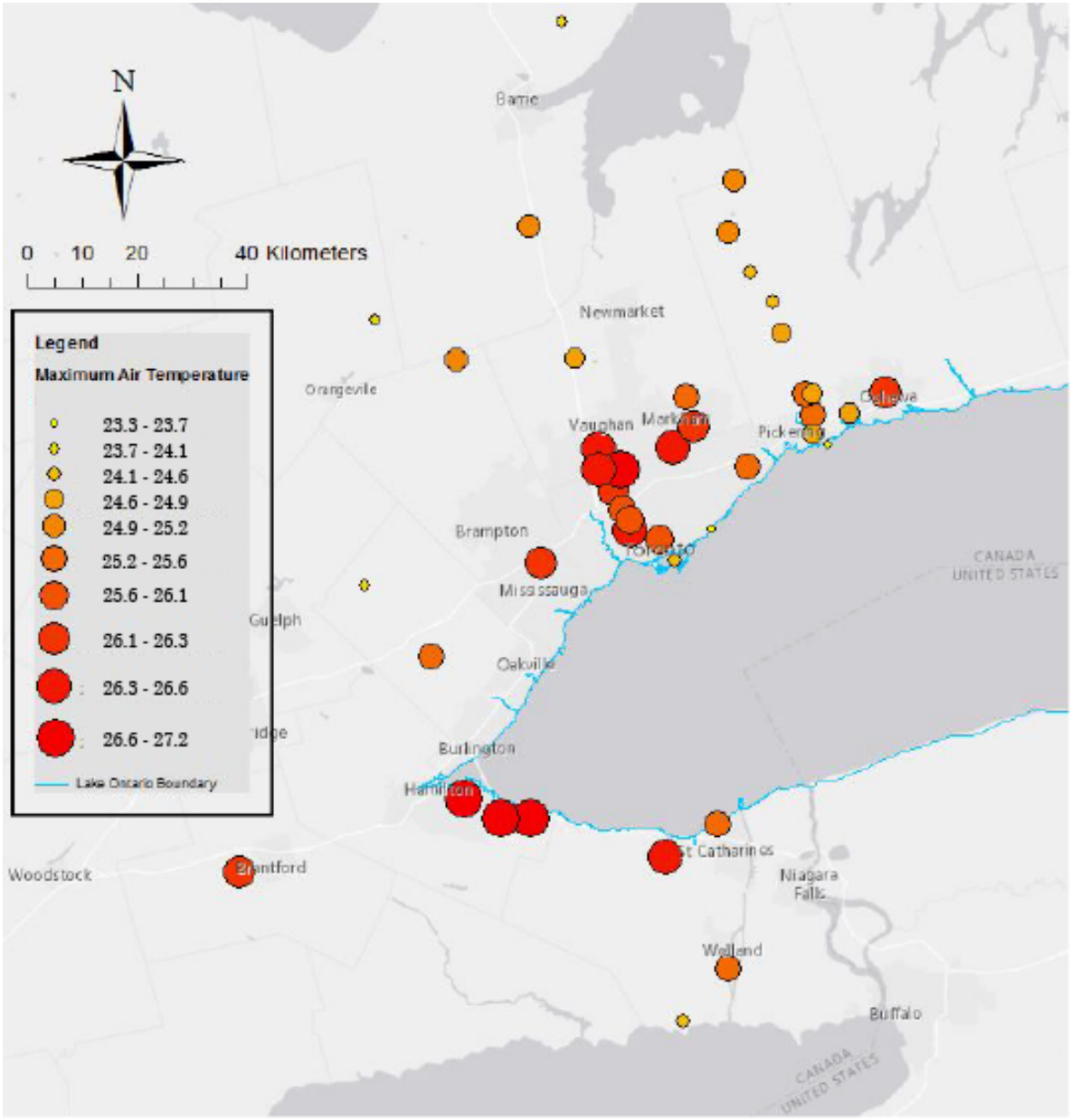

Figure 3.1. Station-specific seasonal summer maximum air temperature averages. Each circle represents an individual station. The color and size of the circle reflects the magnitude of the heat metric, with darker and larger circles indicating higher values.

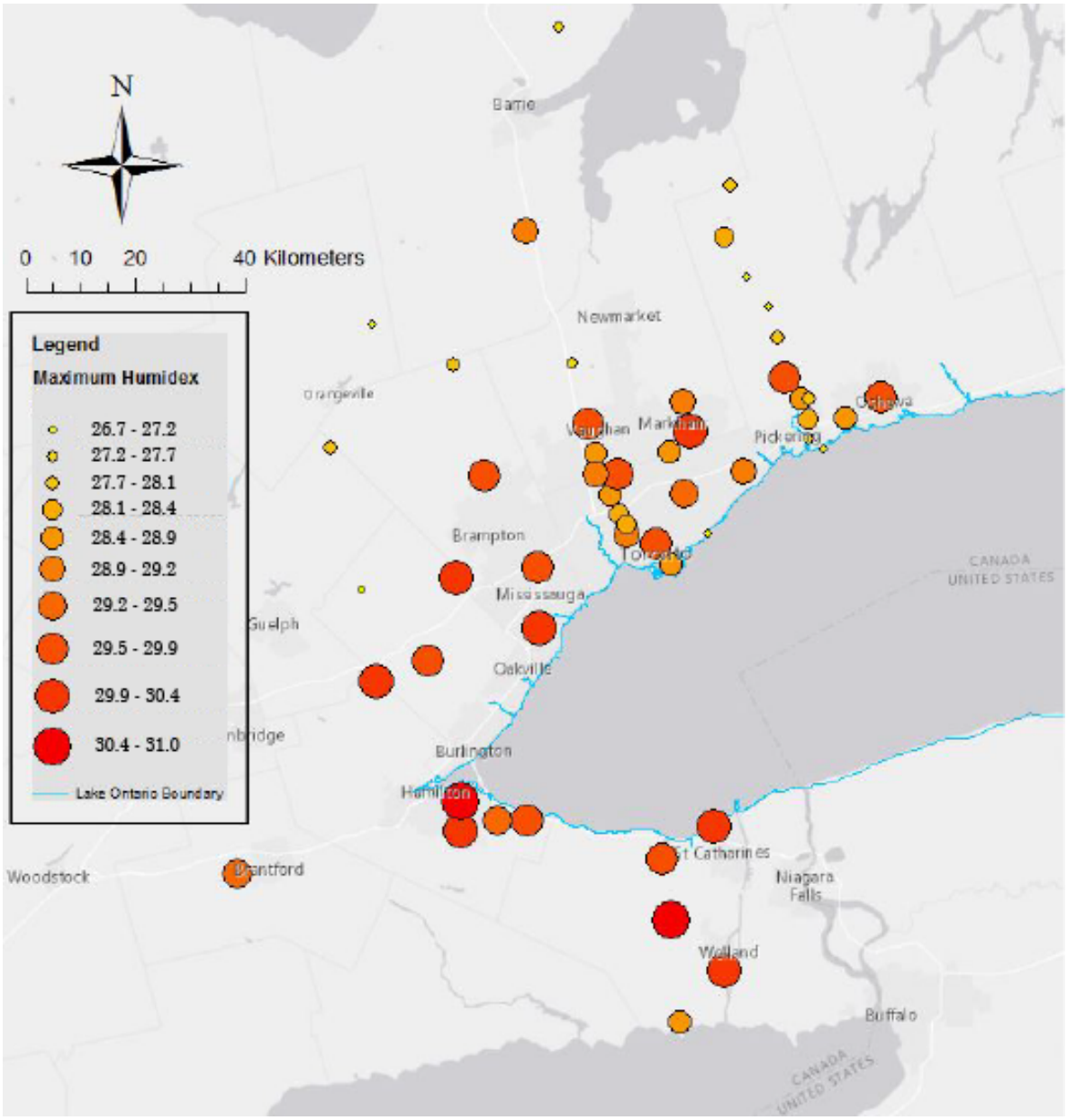

Figure 3.2. Station-specific seasonal summer maximum humidex averages. Each circle represents an individual station. The color and size of the circle reflects the magnitude of the heat metric, with darker and larger circles indicating higher values.

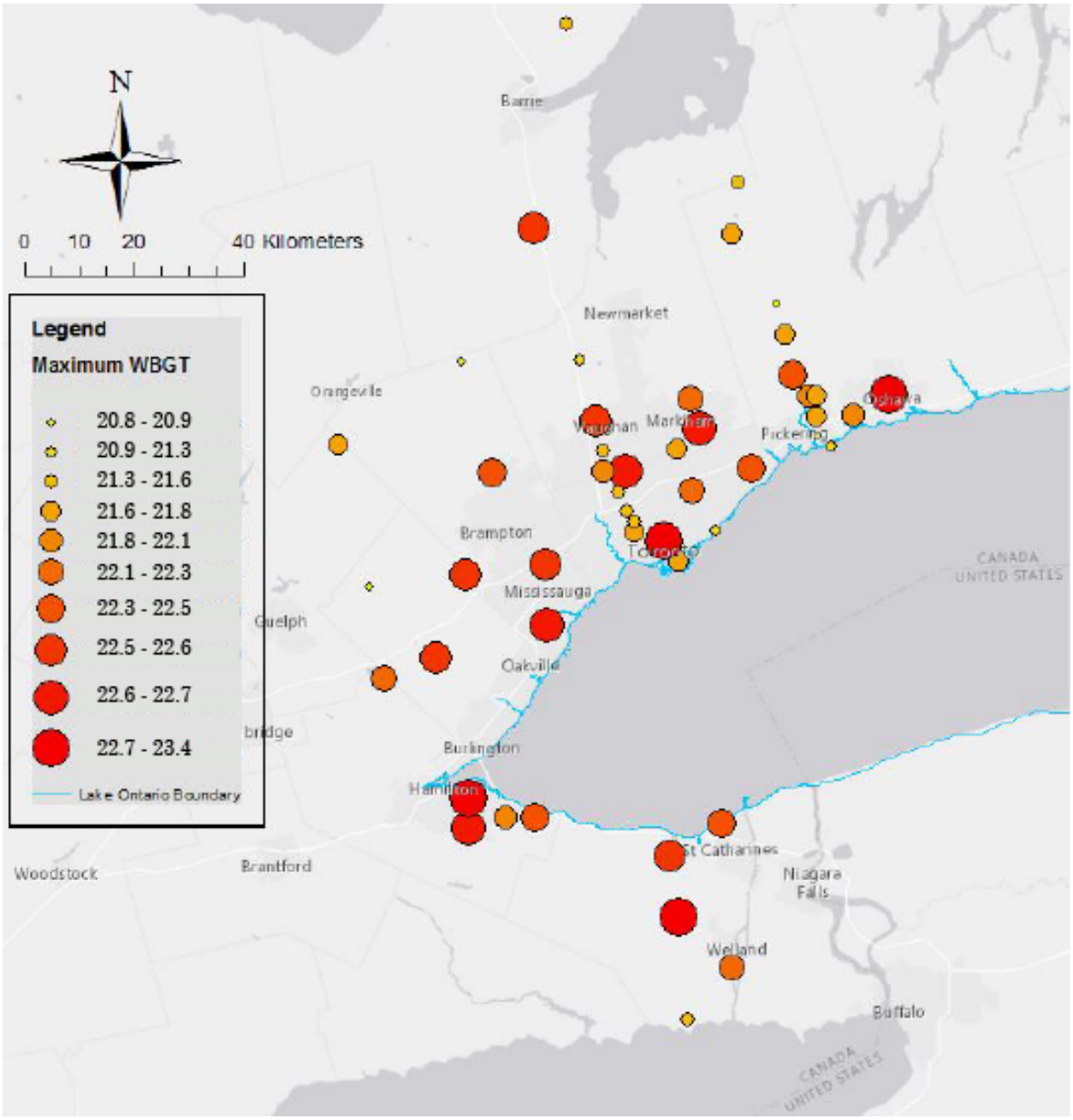

Figure 3.3. Station-specific seasonal summer maximum WBGT index averages. Each circle represents an individual station. The color and size of the circle reflects the magnitude of the heat metric, with darker and larger circles indicating higher values.

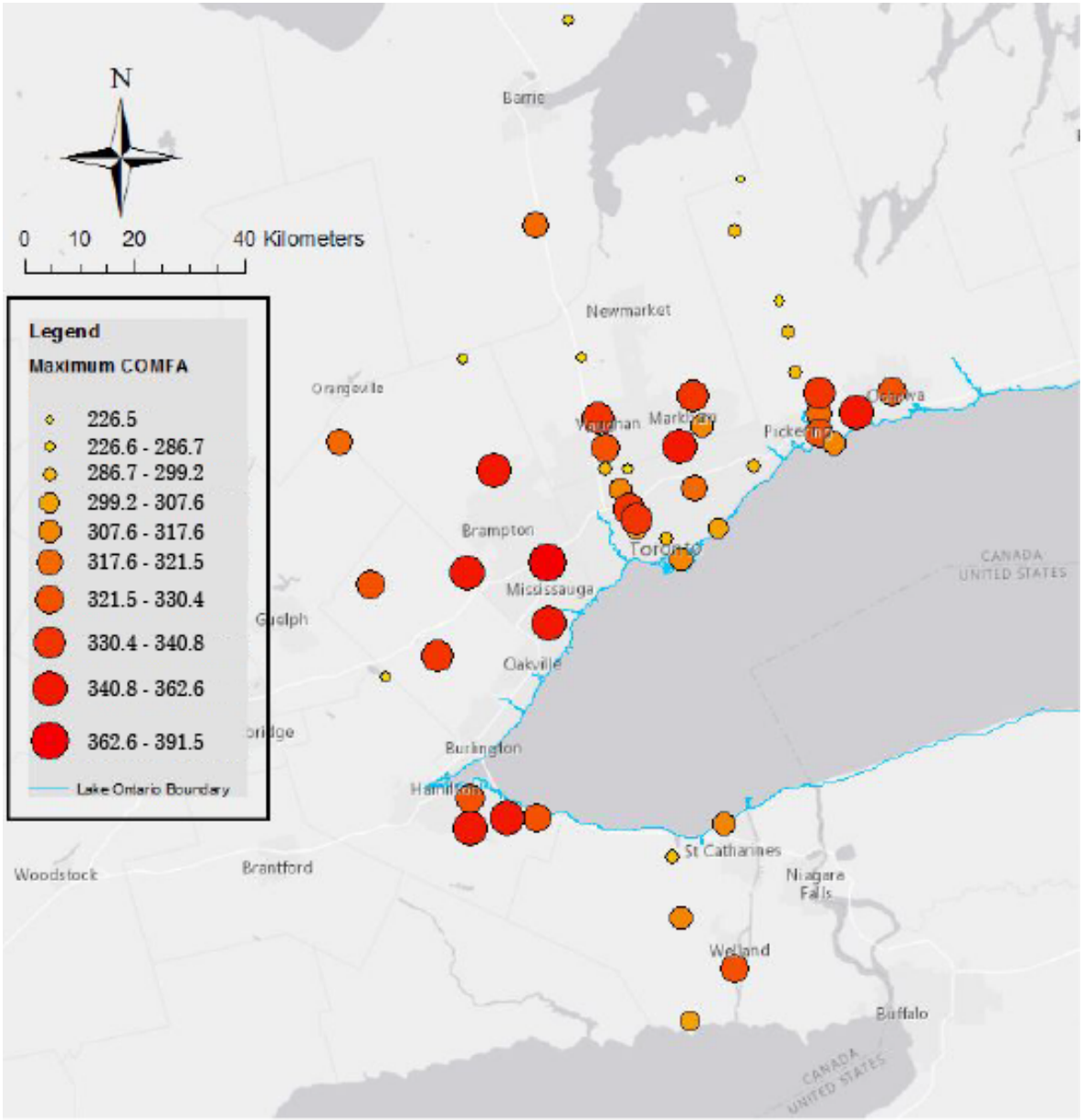

Figure 3.4. Station-specific seasonal summer maximum COMFA averages. Each circle represents an individual station. The color and size of the circle reflects the magnitude of the heat metric, with darker and larger circles indicating higher values.

3.2 EMS Response Calls

Throughout the study period, a total of 11,773 HR and 15,878 NHR EMS response calls were made within the city limits of Toronto. The total number of daily HR EMS calls is plotted in Figure 3.5, which depicts a gradual incline in the daily calls throughout the summer season. Figure 3.6 shows the sex/gender distribution of the HR EMS calls; 5,073 of the EMS calls were for HR illness in males, 5,775 in females, and 925 calls were of unknown sex/gender. Similarly, the age distribution of the HR EMS calls are displayed in Figure 3.7; 273 calls were made for individuals younger than 15 years of age, 5,716 calls for individuals age 15 − 64 years, 4,903 for individuals aged 65 or older, and 881 calls were unknown. The map of the distribution of the HR EMS calls nearest to each station illustrates geospatial variation in the burden of heat stress in Toronto (Figure 3.8). In particular, higher numbers of standardized HR EMS calls can be seen near the stations that are located northwest of the downtown core (Table 2.5).

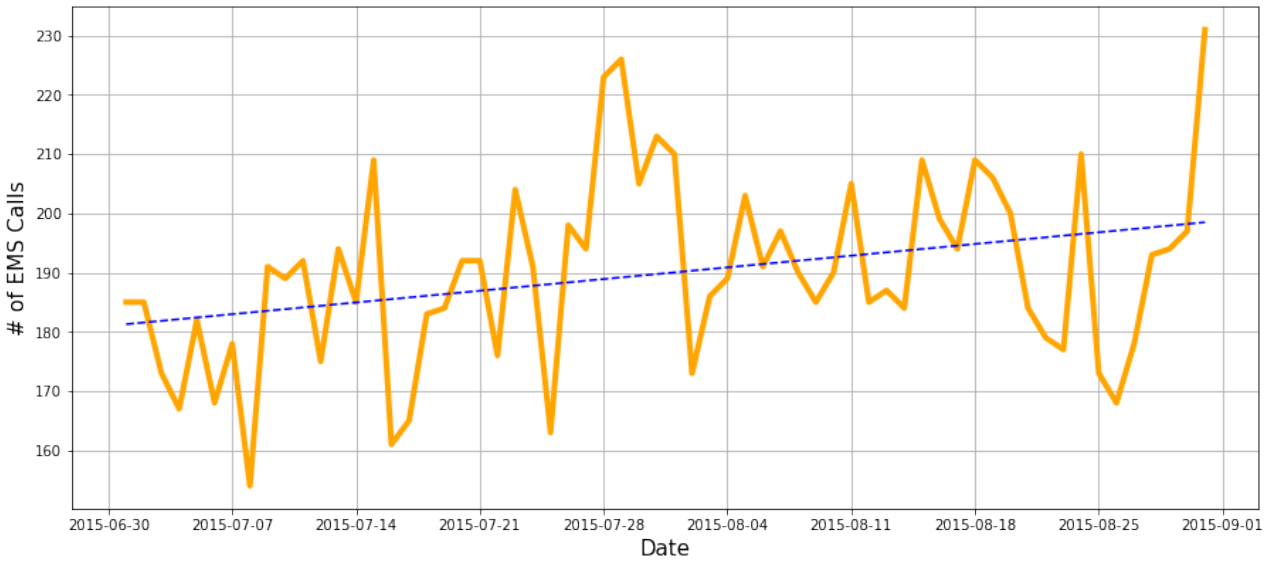

Figure 3.5. Daily heat-related EMS ambulance response call totals over the study period. The dashed blue line represents the linear trend.

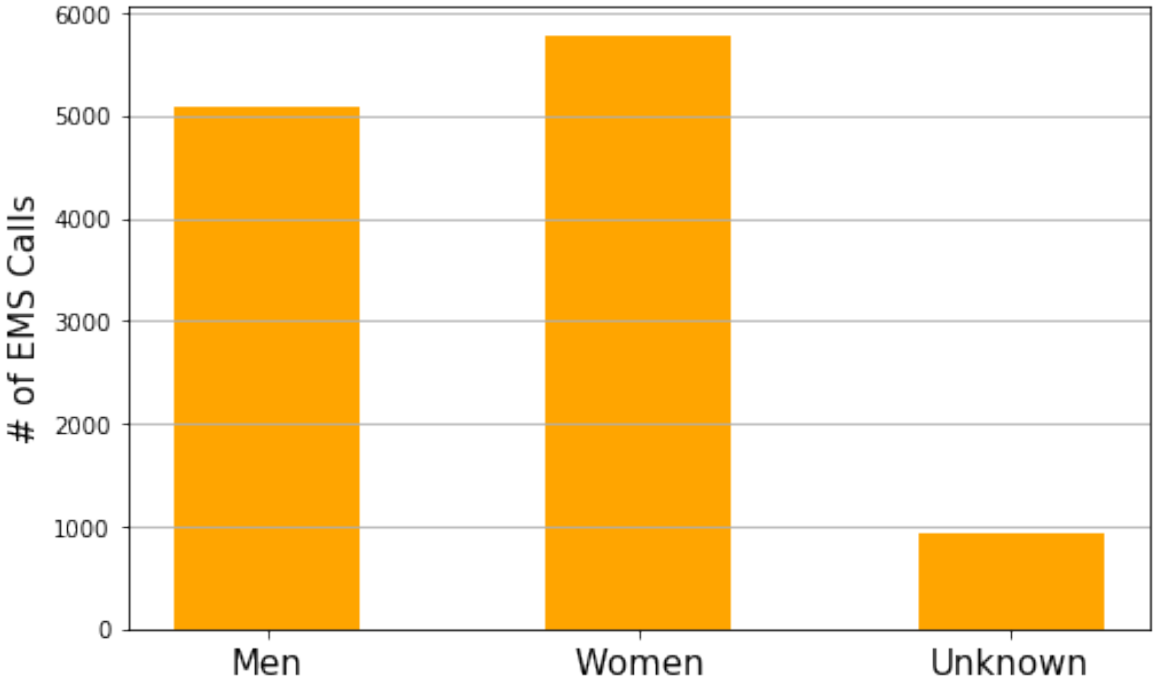

Figure 3.6: Total heat-related EMS ambulance response calls seperated by gender.

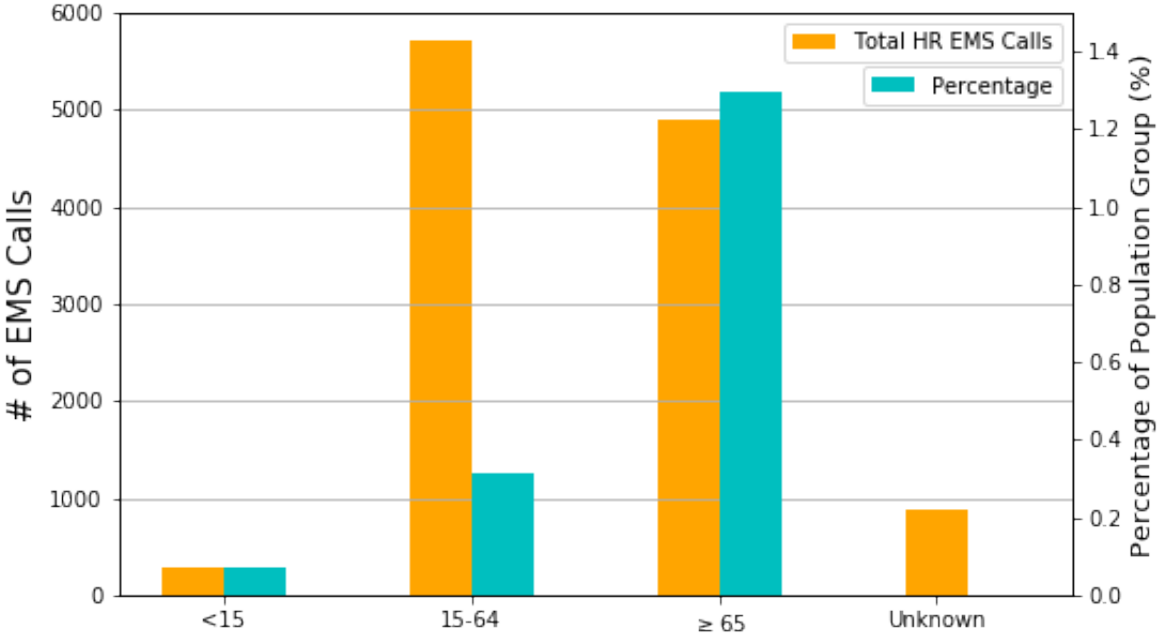

Figure 3.7. Total heat-related EMS ambulance response calls seperated by age (orange columns), with blue columns representing the number of heat-related calls made based on the City of Toronto age group population (2011 Census), displayed in percent.

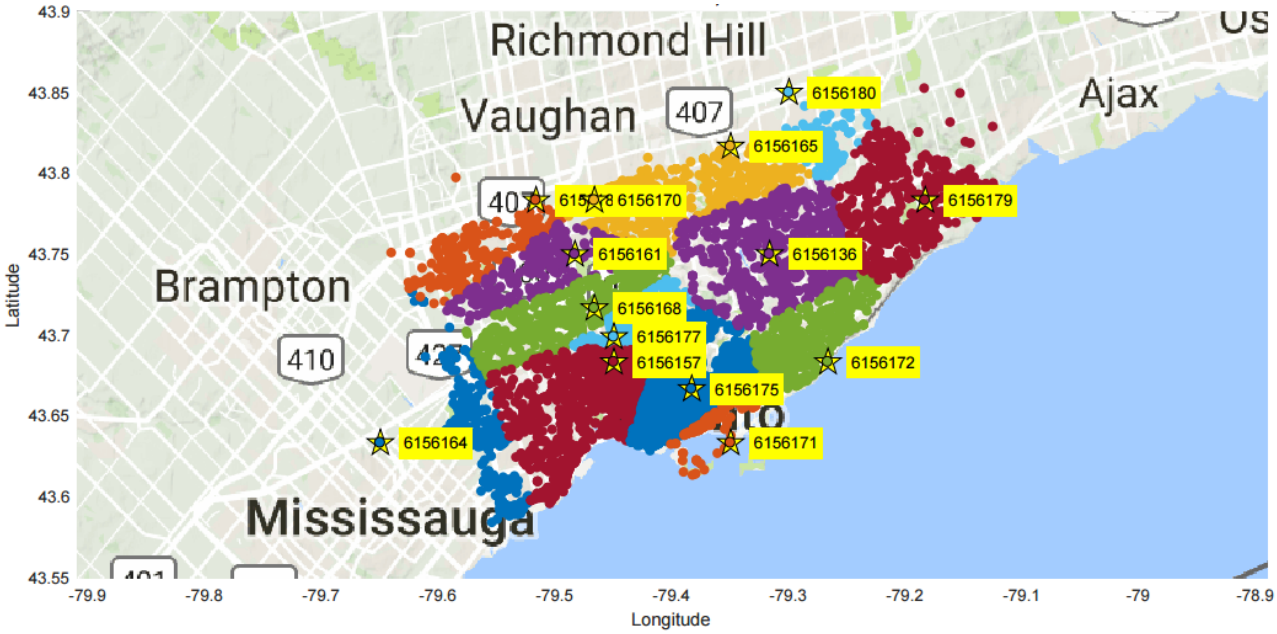

Figure 3.8. Visual representation of the total heat-related EMS ambulance response calls seperated by station. Each color coordinates with one of the 14 mesonet monitoring stations (stars) dispersed within or near the Toronto City limits.

3.3 Heat Metrics, Exposure Proxies, and EMS Response Calls

Table 3.1 displays the calculated values of the slope and variance (R^2 value), with significance of the correlation (p-value) indicated, based on the OLS regression that was applied to the three spatial exposure proxies (airport, averaged- city, and station-specific). Both the slope and variance values gradually increase among all heat stress metrics as the representation of the current meteorological environment moves from a broader-scale representation to a more local-scale representation, indicating that the station-specific spatial exposure proxy provides the strongest relationship between the heat metric values and the number of HR EMS response calls made. Slopes ranged from $0.001 - 0.047$ for the airport proxy, $0.003 - 0.056$ for the averaged-city proxy, and $0.003 - 0.066$ for the station-specific proxy. The slope of the OLS regression for each heat stress metric represents the relative change

in number of HR EMS calls per 1°C or 1 Wm^{-2}. Variances ranged from $0.000 - 0.048$ for the airport proxy, $0.009 - 0.075$ for the averaged-city proxy, and $0.019 - 0.111$ for the station-specific proxy. These slopes and variances show that the station-specific proxy performs systematically better across all heat stress metrics.

The multi-variate analysis identified the COMFA heat stress metric as the most significant predictor of HR EMS response calls for the airport ($R^2 = 0.048$), averaged-city ($R^2 = 0.075$), and station-specific proxy ($R^2 = 0.111$). However, all five heat stress metrics for all three spatial exposure proxies show a weak relationship with HR EMS response calls (maximum $R^2 \leq 0.111$) for the two-month study period. The greatest differences between slope and variance values occur between the airport and station-specific proxies with maximum differences of 0.022 (T_{max}) and 0.063 (COMFA), respectively. The WBGT consistently reported the lowest correlation values with HR EMS ambulance calls. Low slope and variance values are attributable to Toronto's below average summertime temperatures during July and August 2015, further discussed in Section 4.1.

Only when the representation of the meteorological environment for human exposure progressed from broader-scale to local-scale did p-values reveal that specific heat metrics had a significant correlation with HR EMS response calls; the COMFA heat stress metric within the averaged-city proxy and the T_{min} and COMFA heat stress metrics within the station-specific proxy (Table 3.1). Figures $3.9 - 3.11$ display the OLS regression line of best fit and 95^{th} percentile CIs for each heat stress metric for each spatial exposure proxy. For all three spatial exposure proxies, the number of HR EMS response calls steadily rises with increasingly hot, or hot and humid, conditions.

Table 3.1. The OLS regression slope and variance values for each of the three spatial exposure proxies. Significance of the correlation is indicated by an *.

	Airport		Averaged-City		Station-Specific	
	Slope	R^2	Slope	R^2	Slope	R^2
T_{max}	0.020	0.008	0.029	0.016	0.042	0.044
T_{min}	0.047	0.031	0.056	0.039	0.066	0.081*
Humidex	0.002	0.0002	0.024	0.021	0.023	0.031
WBGT	0.001	0.0000	0.025	0.009	0.036	0.019
COMFA	0.002	0.048	0.003	0.075*	0.003	0.111*

3.4 Athlete and Spectator Energy Budget Case Studies

Anecdotal evidence from Environment Canada, Hamilton Paramedic Service, and St. John Ambulance revealed that a combined 10 HR EMS calls were made during the men's bronze medal and women's gold medal soccer matches on July 25th, and that 13 HR EMS calls were made during the men's gold medal soccer match on July 26th. All HR EMS calls were made directly from the Hamilton Soccer Stadium venue. One spectator that attended the men's bronze medal soccer match stated that "*on the way there [the stadium], there were long lines for the shuttle buses, and several people had to be treated for heat stroke*" (Sills, 2017). Similarly, on July 26th on-site paramedics noted that the conditions at the venue were "*very hot*" and that "*multiple calls from different agencies were calling at the same time*" and that they "*had to call in crews to stand-by in hard enclosure [the stadium] due to the call volume*" (Hamilton Paramedic Service, 2017).

The perceived HR EMS calls and anecdotal communication mentioned above are consistent with the heat stress results from the modeled spectator EBs during each of the three soccer matches. Besides for the duration of the game, spectator EBs were also modeled for the hour before and after the game to account for those spectators that arrived early to watch athlete warm-ups and stayed late to watch the medal ceremony. Figure 3.12 displays the temporal changes of the modeled

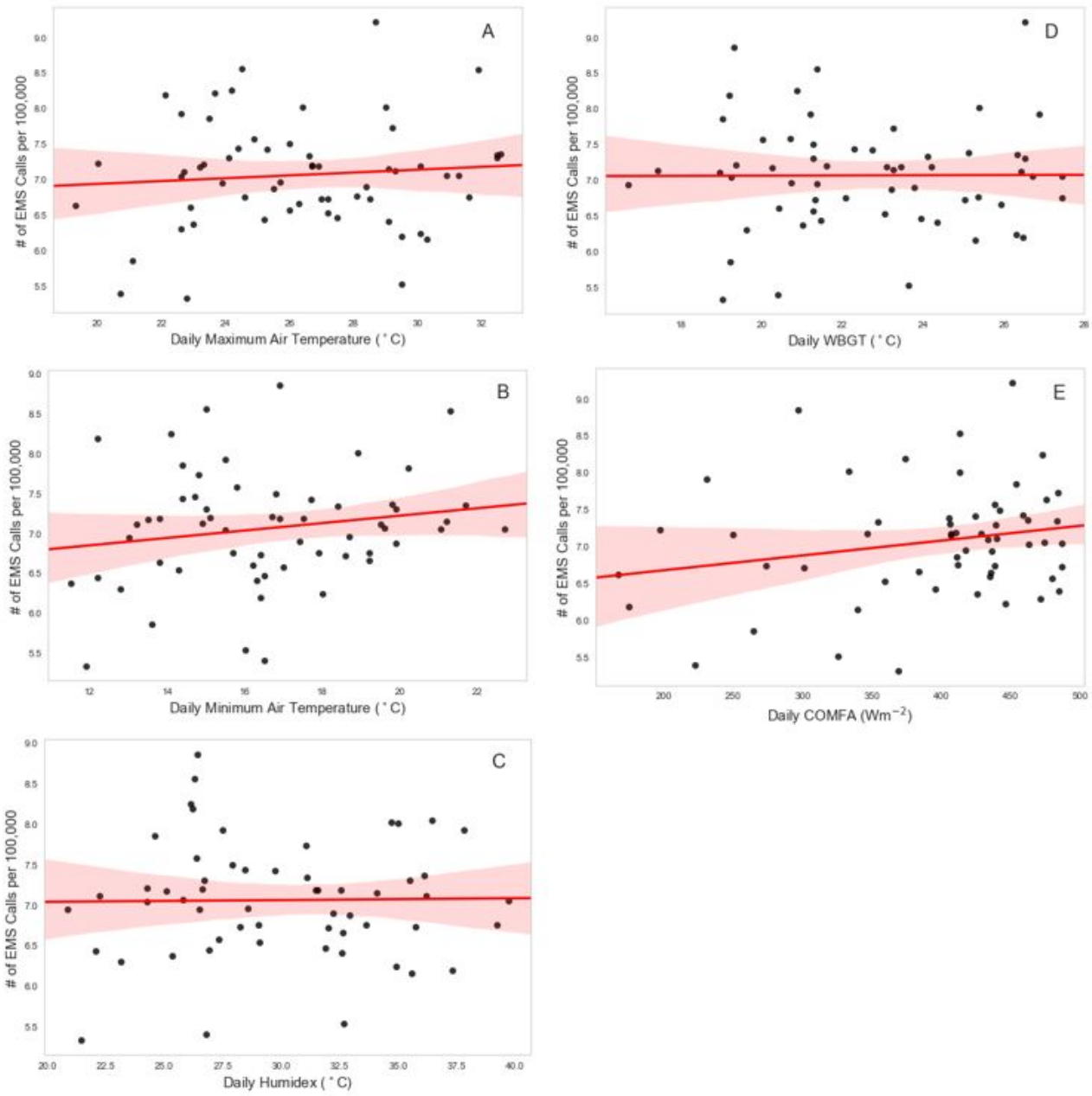

Figure 3.9. Plots of daily heat stress metric values versus the number of HR EMS calls made per 100,000 people for the airport proxy for the daily A) maximum air temperature, B) minimum air temperature, C) maximum humidex, D) maximum WBGT index, and E) maximum COMFA EB. The black circles represent the number of HR EMS response calls at a given heat stress metric value. The linear trendline (red line), which produced the strongest R^2 values, and 95th percentile CIs (red shaded area) are displayed for each heat metric, respectively.

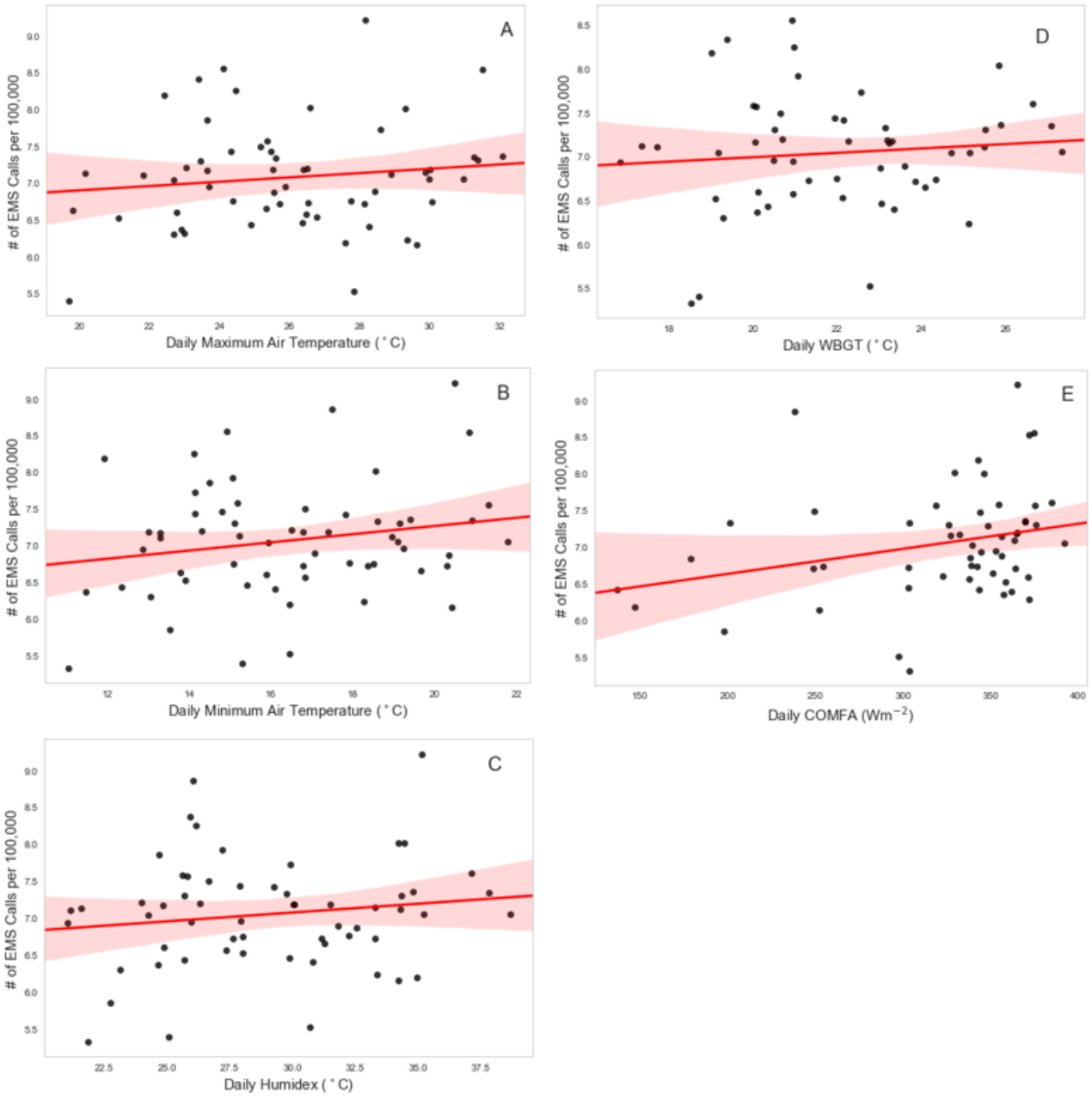

Figure 3.10. Plots of daily heat stress metric values versus the number of HR EMS calls made per 100,000 people for the averaged-city airport proxy for the daily A) maximum air temperature, B) minimum air temperature, C) maximum humidex, D) maximum WBGT index, and E) maximum COMFA EB. The black circles represent the number of HR EMS response calls at a given heat stress metric value. The linear trendline (red line), which produced the strongest R^2 values, and 95th percentile CIs (red shaded area) are displayed for each heat metric, respectively.

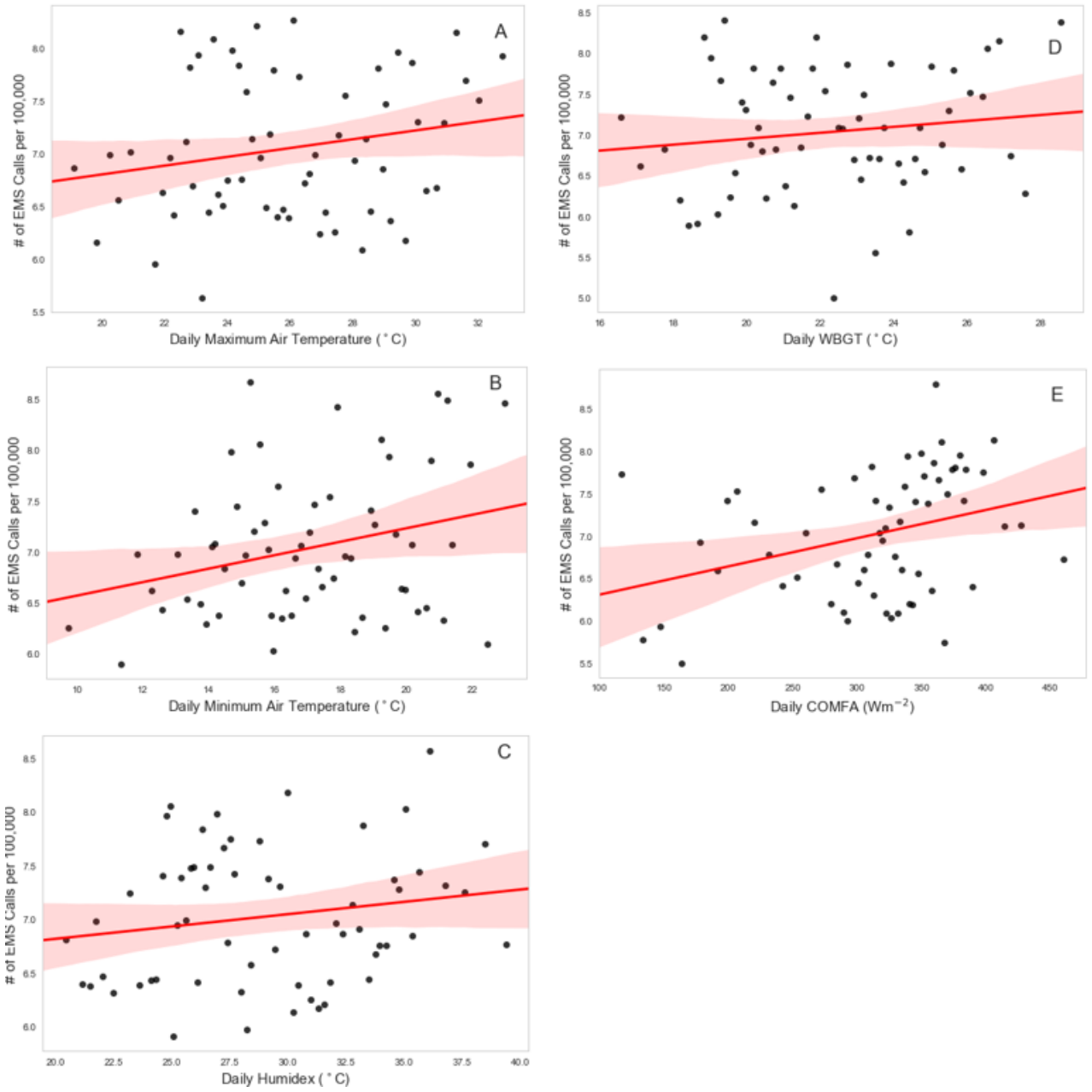

Figure 3.11. Plots of daily heat stress metric values versus the number of HR EMS calls made per 100,000 people for the station-specific airport proxy for the daily A) maximum air temperature, B) minimum air temperature, C) maximum humidex, D) maximum WBGT index, and E) maximum COMFA EB. The black circles represent the number of HR EMS response calls at a given heat stress metric value. The linear trendline (red line), which produced the strongest R^2 values, and 95^{th} percentile CIs (red shaded area) are displayed for each heat metric, respectively.

spectator EBs. The EB results found in the three-match spectator analysis fell within the range of 'neutral' (little threat of heat stress) to 'hot' (dangerous threat of heat stress). EB values ranged from $-26.9 - 277.7$ Wm^{-2} for the men's bronze medal match, $22.41 - 576.2$ Wm^{-2} for the women's gold medal match, and $-55.9 - 243.1$ Wm^{-2} for the men's gold medal match (Figure 3.13). Even with low metabolic rate modeling (M_{act} = 166 Wm^{-2}), the spectator EBs reached well above the 'heat stress zone' (> 121 Wm^{-2}) (Brown and Gillespie, 1986; Harlan et al., 2006), and commonly remained in the 'slightly warm' range (moderate threat of heat stress) or higher for the second half of each soccer event. Overall, a steady increase in EBs throughout the game period is observed for all three matches (Figure 3.12).

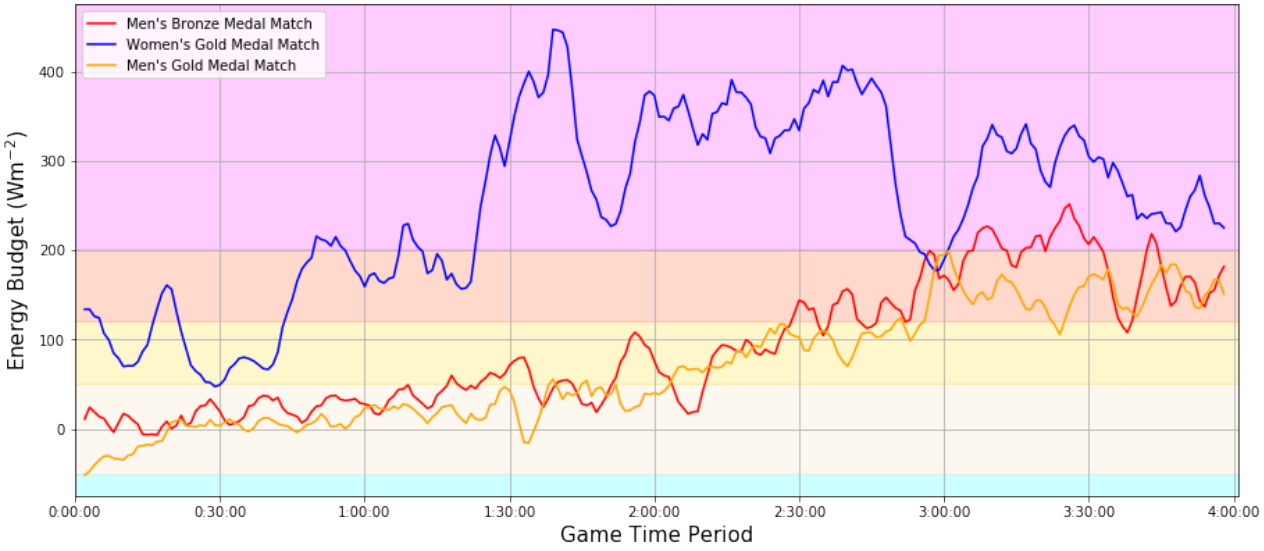

Figure 3.12. Temporal changes of the modeled spectator EBs for each of the three soccer matches. The start and end times of each match are as follows; 13:05 – 15:05 July 25, 2015 (Men's Bronze Medal Match) (red line), 18:35 – 20:35 July 25, 2015 (Women's Gold Medal Match) (blue line), and 13:05 – 15:05 July 26, 2015 (Men's Gold Medal Match) (yellow line). The background colors are indicative of the spectator subjective interpretation to the COMFA EB model output (Table 2.4).

Peak EB values, and therefore the greatest thermal discomfort, occurred during the women's gold medal soccer match (Figure 3.13), where spectators remained in

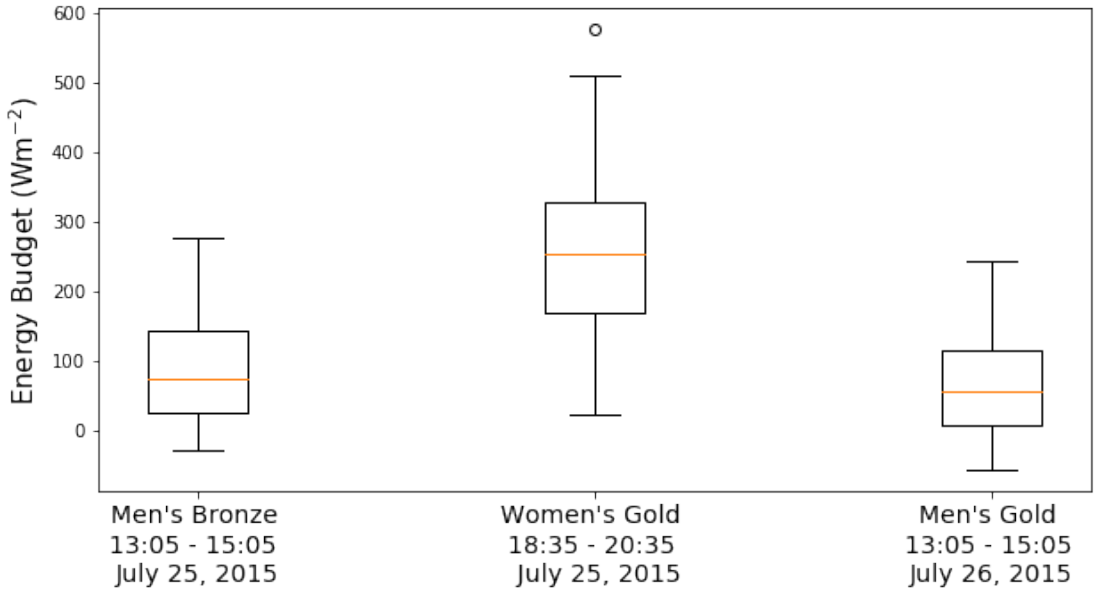

Figure 3.13. Box plot depicting the range of spectator EB values during each of the three soccer matches. The interquartile range (IQR) is indicated by the length of each box plot (25th to 75th percentiles), with outliers marked by °.

the 'hot' range for almost the entirety of the game (7:00pm − 8:28pm LST and 8:36pm - 9:35pm LST) (Figure 3.12). The men's bronze medal match recorded a dangerous threat of heat stress for 27 minutes total mainly from 3:11pm − 3:38pm LST. The most thermally comfortable game was the men's gold medal match, which only exceeded the 'hot' threshold for 2 minutes from 3:18pm − 3:19pm LST. However, as the majority of HR EMS calls were made during the men's gold medal match, this result emphasizes that mass gatherings have the ability to enhance heat stress and thus the number of HR illnesses occurring at lower EB levels. The temporal changes in the EB streams that produce the final spectator EB (based on Equation 2.3) for each of the three events are shown in Appendix C. The EB for the spectators follows a pattern strongly related to the plotted R_{abs} because of relatively constant M_{act}, C, E, and L_{emit}.

Athlete EBs were modeled for the duration of the game and the hour before to

account for pre-game warm-ups, with the assumption that the athletes remained outdoors during the half-time break. Figures 3.14 − 3.16 display the temporal changes of the modeled athlete EBs for the men's bronze medal match, the women's gold medal match, and the men's gold medal match, respectively. All three player position's had very similar EB values for each of the soccer events. A two-sample t-test confirmed that only the midfielder and goalie EB values for the men's bronze and gold medal matches were significantly different from one another. During the women's gold medal match, all three players endured 'hot' EB levels for the whole game (6:35pm − 8:35pm LST), whereas the men's bronze and gold medal matches reported a dangerous threat of heat stress primarily during the second half of the game (2:15pm − 3:05pm LST).

The dip in player EB values approximately two hours into each soccer event can be attributed to the approximately 20 minute half-time break, when players generally sit and a decrease in M_{act} occurs. The temporal changes in the EB streams that produce the final athlete EB (based on Equation 2.3) for each of the three player positions for each of the three events are shown in Appendix D. The EB follows a pattern strongly related to the plotted M_{act} for the men's bronze and gold medal match, and to the plotted R_{abs} for the women's gold medal match. These results are primarily due to a larger variance in wind speeds during the women's gold medal match, which causes R_{abs} to vary more (based on Equation 2.5).

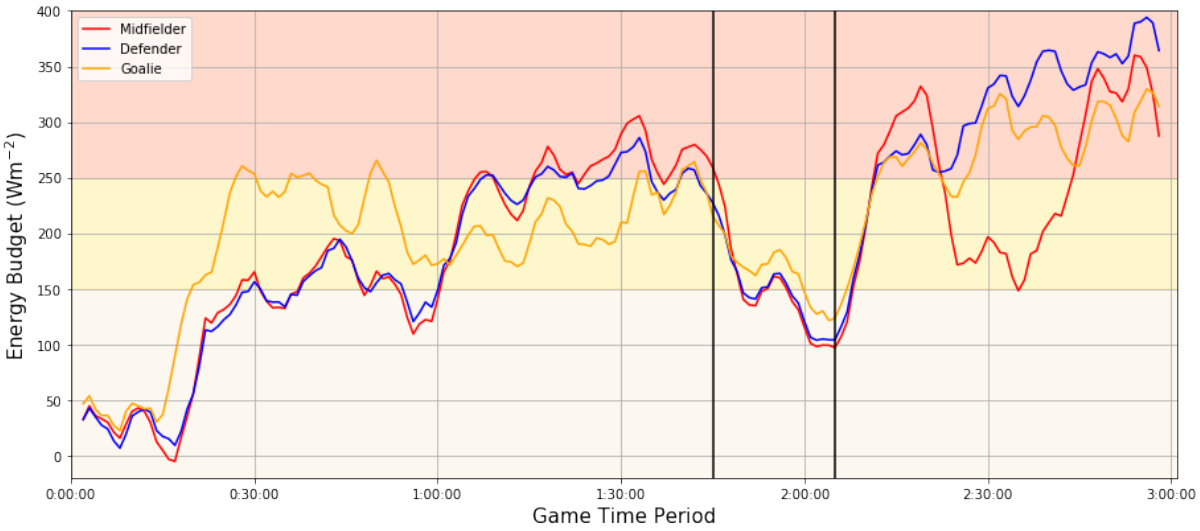

Figure 3.14. Temporal changes of the modeled athlete EBs for each of the three player positions for the men's bronze medal match. The start and end time of the match is 13:05 – 15:05 July 25, 2015, with the half-time break start and end times designated by black vertical lines. The background colors are indicative of the athlete performing physical activity subjective interpretation to the COMFA EB model output (Table 2.7).

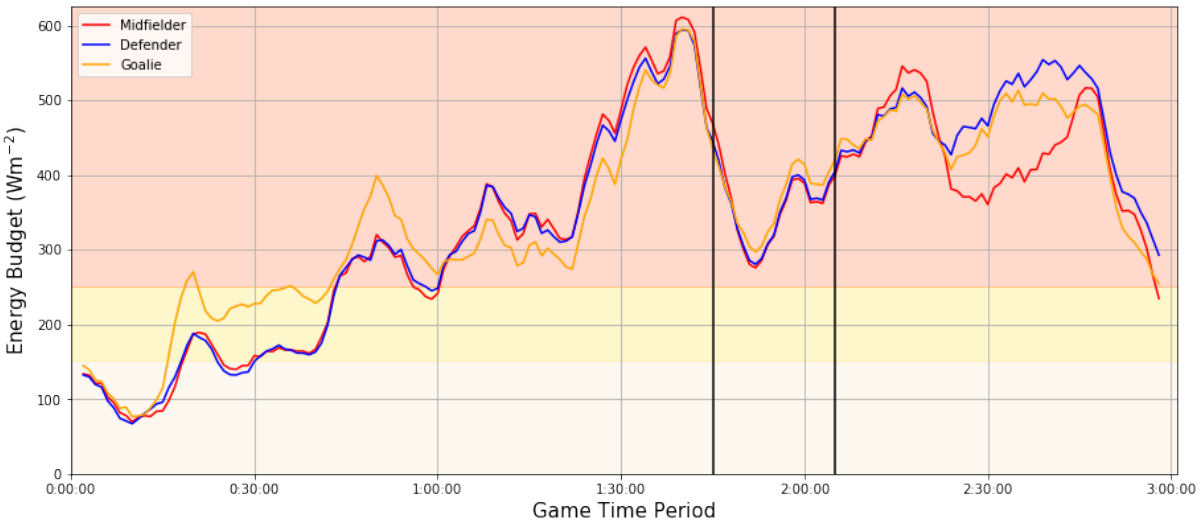

Figure 3.15. Temporal changes of the modeled athlete EBs for each of the three player positions for the women's gold medal match. The start and end time of the match is 18:35 – 20:35 July 25, 2015, with the half-time break start and end times designated by black vertical lines. The background colors are indicative of the athlete performing physical activity subjective interpretation to the COMFA EB model output (Table 2.7).

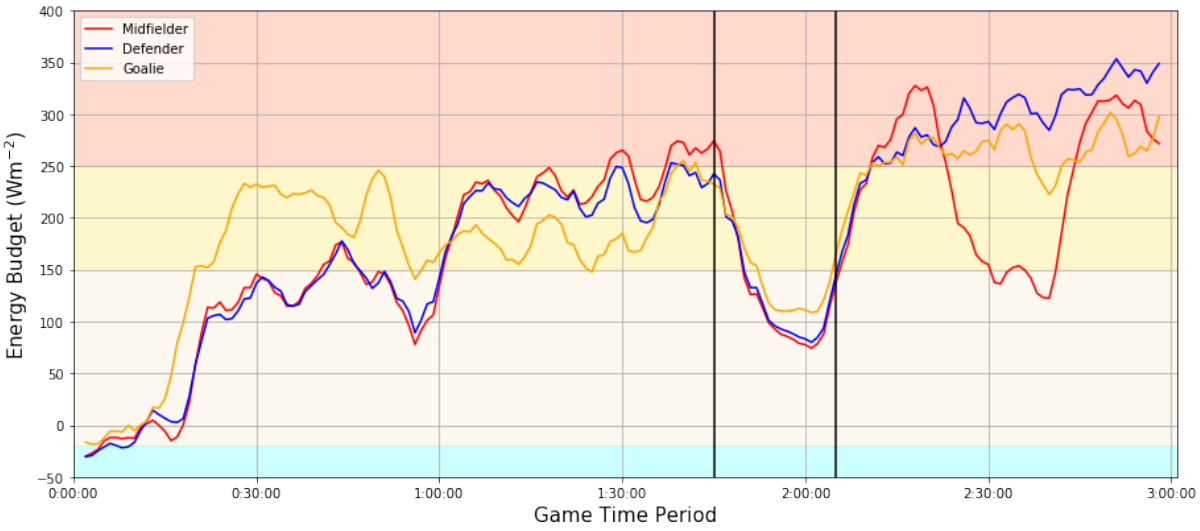

Figure 3.16. Temporal changes of the modeled athlete EBs for each of the three player positions for the men's gold medal match. The start and end time of the match is 13:05 − 15:05 July 26, 2015, with the half-time break start and end times designated by black vertical lines. The background colors are indicative of the athlete performing physical activity subjective interpretation to the COMFA EB model output (Table 2.7).

CHAPTER 4
DISCUSSION

The present thesis aimed to highlight the ability of fine-scale intra-urban meteorological mesonet stations to better predict the human heat-health response at specific environmental conditions in Toronto, Canada and surrounding areas. Results presented provide new information on the potential benefits and uses of such mesonet systems during large-scale events. These new benefits and uses can improve our understanding of the variability among common heat stress metrics in relation to intra-urban heat-health burden to enhance Toronto's resilience to extreme heat, with a focus on mass gathering sporting events.

4.1 Geospatial Station Summertime Averages

Through mapping the heat metrics across the city for summer-time averages, low variability was found in the between-station values for T_{max}, humidex, and WBGT index. Such small spatial heterogeneity indicates that differences in the LCZ and surface cover among stations had little effect on heat stress metric values. Since Toronto experienced below average temperatures during the summer of 2015 (Environment Canada, 2016), favorable conditions for the existence of a heatwave occurred less frequently and the intensity of the UHI was likely smaller, such as what occurs during the winter season (Klysik and Fortuniak, 1999), which in turn presumably limited the distinct signatures of intensity of heat and intra-urban variability within the GTA. Another reason for this low variability may be that the meteorological dataset was not of sufficient length, with no anomalous hot or cold days, to present a wider variance among stations. However, geospatial map results show that the UHI effect is prevalent in both Toronto and Hamilton when looking

at the variation in average summertime T_{max} station values (Figure 3.1). Oke and Hannell (1970) have shown that the local steel works in Hamilton, Ontario is responsible for producing its own UHI. Similarly, Blair (2006) found that within the Toronto-Hamilton urban airshed, meteorological data indicated that two large UHIs are present in the downtown areas of Toronto and Hamilton.

The larger range of summer-time average COMFA values can be attributed to the model's dependence on several environmental and physiological variables as compared to the direct metrics, which adds information that may increase the value for small-scale studies where fine-scale weather and personal information is available (McGregor and Vanos, in review), but also adds complexity. Therefore, the COMFA EB model results are more appropriate when the model is applied to calculate the heat stress experienced by humans at events of short duration rather than over an entire season (e.g., see Brown and Gillespie, 1986; Kenny et al., 2009a,b; Vanos et al., 2012a,b,c).

Overall, the spatial maps across the GTA demonstrate the capability of a mesonet monitoring network to show variations by heat metric and to identify different areas of escalated risks for HR illness. All heat metrics employed in this study were in agreement that the area of the GTA with the greatest escalated risk for HR illness is Hamilton, Ontario, and therefore EMS personnel should concentrate resources in this area during days of excessive heat. The implementation of a mesonet monitoring network in any city can ensure the creation of such geospatial maps, which can be used to inform city public health officials and/or urban planners of areas of increased heat exposure at a finer intra-urban scale during the summer season (Muller et al., 2013; Resch et al., 2011). One particular application of these geospatial maps is the prioritization of hot spot locations for the delay of electricity shut-offs by energy policy managers (Luber and McGeehin, 2008).

Previous studies, with similar goals, that have used remotely-sensed surface temperatures to infer hot spots have stated that providing data at a higher spatiotemporal frequency should be integrated into public health practice and will be more useful for city and county level authorities (White-Newsome et al., 2013). Ng (2012) further expressed that urban climatic spatial information is best understood by urban planners and governments when the information is presented visually. Thus, the geospatial heat maps created in the current research may be extremely valuable for translating research to practice. Companies, such as WeatherBug, currently utilize weather monitoring networks' data for informed decision-making regarding energy efficiency, crop production, public safety, security, transportation and many other critical functions (Anderson and Usher, 2010). In this regard, a robust weather observing network is part of the vital infrastructure needed for modern society.

4.2 Mesonet Monitoring and Human Exposure

This study was the first of its kind to employ within-city weather and EMS response call data that also provided data at high temporal rates. Related studies assessing the connection between heat and health often use one or a low number of stations (Vanos et al., 2012c; Hartz et al., 2013; Graham et al., 2016; Niu et al., 2016; Ng et al., 2013). However, spatial incongruence can exist when we apply a point based attribute to an entire area, which in heat research is entitled exposure misclassification (Kuras et al., 2015; Kuras et al., 2017; Bernhard et al., 2015). By having more stations present in an urban area, we can more accurately assign exposures to a health outcome. This was shown in the current study by the enhanced relationship between the five heat metrics and HR EMS response calls when employing the station-specific method. Furthermore, more spatially-available

data in real or near-real time to assess the relationships between heat and human health is needed to ensure correct classification of the weather conditions present at the location and time an individual succumbs to heat stress and requires medical attention. The rapid growth and continued expansion in the number of automated weather stations and networks can be viewed as a positive step toward expanding data available for this type of applied meteorological research and service (Meyer and Hubbard, 1992). Thus the use of this advanced exposure classification method should be given consideration, especially in cities where 66% of the world's population is projected to reside by 2050 (United Nations, 2014), if mesonet monitoring network resources are available.

The minimal incremental improvement in heat-health response and strength of the relationship when downscaling from the airport proxy to the averaged-station proxy to the station-specific proxy, however, suggests that the need for such local-scale data may not be necessary in moderate weather with no heat waves and little variation. We hypothesize that these relationships would be stronger in a summer with warmer temperatures and heat waves present due to the fact that heat-related EMS response calls were used as the response variable. Furthermore, research is needed to test the station-specific exposure-response method over a longer time-scale to see if similar results arise. Benefits of the localized stations also included connecting the timestamps of each call to each heat metric timestamp. Most studies use the daily values (Hartz et al., 2013; Cheng et al., 2016), yet with a mesonet containing highly resolved temporal information, there is value in exploring intra-daily response.

4.3 Benefits of Station-Specific Proxy for Urban Heat-Health Studies

Observations from July and August 2015 show a gradual incline in the number of heat-related EMS response calls with increasingly higher heat values across all five heat stress metrics (Figures 3.9 - 3.11). This result provides an indication that EMS response calls are reflecting the health burden effects of heat in the city of Toronto. Similar results were observed by Dolney and Sheridan (2006) and Graham et al. (2016), who found that the number of ambulance calls increases by 10% and 12.3%, respectively, during heat events in Toronto. Heat-related EMS response calls were significantly correlated with the T_{min} and COMFA heat metrics, with COMFA being identified as the most important variable in the multi-metric OLS regression analyses. The finding that high T_{min} may create thermal stress to urban residents, often being correlated with excessive heat-related morbidity and mortality (Miralles et al., 2014; Black et al., 2004), is not a new concept. For example, when analyzing the impact of weather on human mortality in multiple U.S. locations, Kalkstein and Davis (1989) determined that warm conditions overnight relate to the highest mortality in summer. Additionally, Goodman et al. (2004) found a 0.4% increase in total mortality associated with a 1°C increase in daily T_{min} from $1980 - 1996$ in Dublin, Ireland. The significant correlation observed between T_{min} and heat-related EMS response calls in the current study advocates for the use of real-time T_{min} when implementing a heat-health warning system within a city.

The COMFA metric was found to be the strongest predictor of heat-related illness in this study. With respect to the COMFA energy budget values, a study by Vanos et al. (2012c) also observed that heat-related EMS response calls were significantly dependent on the COMFA EB estimations of human TC within-city station data in Toronto. However, as Vanos et al. (2012c) only used 1 nearby station to infer weather conditions, the findings of the current study are much more

robust having used data from 14 stations. This significant dependence is likely due to the fact that many studies have both tested and incorporated revisions into the COMFA EB model to ensure maximum agreement between tested subjects environment-based TC and the budget output (Brown and Gillespie 1986; Kenny et al. 2009a,b; Vanos et al. 2012a,b,c). In addition, as the only rational metric employed in this study, the COMFA metric considers all processes pertaining to the body's heat generation and heat transfer with the environment, which are quintessential components to estimating heat stress (Havenith and Fiala, 2015). The R_{abs} load is often the largest contributor to human heat gain and TC in warm conditions (Johansson et al., 2014; Kantor et al., 2014; Taleghani et al., 2015; Kenny et al., 2008), and the M_{act} load is often near or above the R_{abs} load when a human is exercising (Brotherhood, 2008; Casa et al., 2015). Thus, this study suggests that outdoor EB modeling has the potential to be a used as a guidance tool for heat-related illness prediction by EMS resources and application in bioclimatic urban planning and design to reduce vulnerability to heat stress (Brown et al., 2015).

The humidex and WBGT index had the lowest correlation with HR EMS response calls. This result is consistent with some of the WBGT index limitations underlined by Budd (2008): notably the fact that the metric does not adequately reflect the heat stress experienced by a human in a very humid and stagnant air flow environment when the evaporation of sweat is restricted. Originally designed to control heat-related illnesses in military physical training camps, D'Ambrosio Alfano et al. (2014) found that WBGT index values do not vary linearly with M_{act}, which questions whether the WBGT index is appropriate for heat stress assessment of a human not performing physical activity. Currently the WBGT index is used primarily to monitor environmental conditions during high metabolic activities such

as occupational labor, military training, and athletics, with activity modifications dependent on the type of activity and index output (see Table 2.2) (Armstrong, 2007). Moreover, the WBGT index output ranges used to indicate heat stress are not designed for the average person engaging in everyday activities. Further research is needed to create accurate WBGT index thresholds for the average person. The humidex, while a 'perceived temperature', does not take into account spatial variations in radiation or wind speed, like the WBGT index and COMFA, which are fundamental components of heat stress analysis (Brown and Gillespie, 1995).

Another solution to the low correlations observed by the WBGT index (and the COMFA EB model) could be the errors associated with estimating the radiation experienced by a human through the use of the globe thermometer. According to the literature, these errors regularly occur due to three main characteristics of the globe thermometer; 1) shape and size (Johansson et al., 2014; Kantor and Unger, 2011; Thorsson et al., 2007), 2) color (Johansson et al., 2014; Kantor and Unger, 2011; Kenny et al., 2008; Montieth and Unsworth, 2008), and 3) material (Budd, 2008; Johansson et al., 2014; Kantor and Unger, 2011; Kantor et al., 2014). Considering that the human physical appearance replicates a cylinder with an average albedo between 0.33 and 0.40 (Kenny et al., 2008), the spherical shape, small size (150mm), and black matte color of the globe thermometer, often limiting the approximation of R_{abs} to a seated person and overestimating the solar component of R_{abs}, does not correctly resemble a human. Additionally, the heavy copper material (0.4mm thickness) of the globe thermometer regularly causes a slow response time (approximately 20−30min) to record an accurate R_{abs} value, which maybe affects the ability to predict R_{abs} in shorter timescales, and misses the influence of intermittent clouds.

4.4 Heat Stress at Sports Events

The anecdotal evidence from spectators, Environment Canada employees, and paramedics alike regarding the heat stress experienced during the soccer matches that took place on July 25th and 26th demonstrates that EMS personnel may have been unprepared to handle the vast influx of HR illness complaints recorded at the Hamilton Soccer Stadium venue. With both spectator and athlete EBs exceeding the 'hot' subjective interpretation threshold for all three matches, venue modifications on such days should be considered for the soccer stadium and other outdoor facilities that intend to hold mass gatherings in Hamilton, Ontario. For example, venue modifications could include field-surface-type transition from synthetic turf to natural grass, as the radiational properties of such surfaces affects both the air temperature and the interactions of total radiation fluxes with the human body within a microclimate (Hardin and Vanos, 2017), and/or the addition of shade sails over top of the stadium and fans to support air flow. Brown (2011) emphasizes how design modifications to outdoor environments can improve TC and can save lives in extreme cases.

Such modifications could greatly impact short-term TC during sports events since the temporal changes in the EB streams show that the final EBs are strongly influenced by a combination of the R_{abs} and M_{act}. Again this result emphasizes the need for a better measurement of the total R_{abs} by a human in an outdoor environment by use of some method other than the globe thermometer. Without the mesonet station on site, spectator and athlete EB analysis would not have been possible. In the women's gold medal match, where both spectator and athlete EBs climbed rapidly into the upper levels of the 'hot' range, attendees experienced the greatest levels of R_{abs} and, therefore the highest levels of thermal discomfort. No other study has yet to apply EB modeling to spectators at a sporting event,

however, such a method may become more important at large-scale sporting events in hot-humid climates in the coming years, such as the 2020 Summer Olympics in Tokyo, Japan and the 2022 FIFA World Cup in Qatar (Matzarakis and Frohlich, 2014; Sofotasiou et al., 2015; Tsunematsu et al., 2016). Matzarakis and Frohlich (2014) specifically express that a large-scale sports event in Qatar may be harmful for unacclimatized visitors, if the event takes place during months with extreme heat conditions, and suggest the winter months as a more appropriate time when thermally comfortable conditions are more common.

The athletes endured the highest EB rates overall leading studies like that by Casa et al. (2015) to recommend that public health officials, to maximize athlete safety and performance, establish on-site emergency response plans for venues (like Hamilton Soccer Stadium) that are located in hot spot areas. Yet, often times at mass gathering events it is the larger spectator volumes that can lead to potentially higher patient volumes (Milsten et al., 2003). Considering that the V_w values recorded by the mesonet station placed in open air just outside Hamilton Soccer Stadium (see Figure 2.4) were used as inputs to calculate the total EBs, it can be assumed that the heat stress experienced by the spectators in the stadium was likely higher than calculated due to limited air flow in the crowded stands. Additionally, the orientation of the stadium, with stand-seating facing directly east and west, likely caused the spectators sitting in the west-facing stands to experience more heat stress than others due to the great amount of solar R_{abs} from the setting sun during the event. We do not know where most of the EMS calls came from at the stadium so we can only speculate that more may have come from the west-facing stands.

Kenny et al. (2008) and Vanos et al. (2012a) similarly emphasize that radiation is an important variable to consider in outdoor TC research since R_{abs} is commonly the largest contributor to the human EB equation and has a strong negative

relationship with human TC. Many studies have suggested that reducing R_{abs} by increasing the shade over a structure and implementing natural surfaces will have a positive effect on human TC and heat health and will reduce summer temperatures (Graham et al., 2016; Vanos et al., 2016; Giannakis et al., 2016; Perini and Magliocco, 2014; Vanos et al., 2012c). Vanos et al. (2012c) explains that the sensitivity of the COMFA EB output to R_{abs} variations should influence the installment of more urban weather stations to improve spatial modeling of hot spots which will serve as a guide to EMS deployment resources. Positioning such EMS deployment resources in hot spot areas during episodes of hot weather and/or large-scale events and providing sufficient staffing for those resources are both vital strategies for reducing HR illness cases (Dolney and Sheridan, 2006). In preparation for the 2020 Summer Olympics in Tokyo, Japan that will take place during Tokyo's hot and humid summer, potentially exposing attendees to the most challenging weather conditions ever observed in the modern history of the Olympic Games, city officials should seriously consider the development of a health and weather mesonet monitoring package that would encompass monitoring and prediction products focused on heat stress. Like at the Games, it would be beneficial for attendees to be able to access weather data from the nearest mesonet station on their smart phone at the Olympics to influence behavior and decision-making by an individual to take the necessary precautions to avoid succumbing to heat illness.

4.5 Limitations and Future Recommendations

As with all scientific research, there are limitations to this study. These limitations involve finite observational weather data, possible TEMS response call mis-diagnosis, and deficiency of socio-economic, demographic, and geographic human information, all of which will be discussed in more detail herein.

4.5.1 Mesonet Monitoring Data

A few mesonet monitoring network stations, assembled by the MSC of Environment Canada in preparation for the Games, began collecting data in May 2015. However, the full array of stations were not completely operational until the beginning of July 2015. Additionally, the gradual decommission of the stations began in September 2015. As a result, the meteorological dataset used to accomplish the objectives of this study was limited to only 2 months of data (July and August 2015) in order to incorporate data from all 53 stations. A study that utilizes a small dataset has a reduced chance of detecting a true effect estimate and a reduced likelihood that a statistically significant result reflects a true effect due to wide confidence intervals. The consequences of this often include over- or underestimations of the effect size and low reproducibility of results. Knowing this, Environment Canada should consider the permanent operational reinstatement of all 53 mesonet stations to construct a real-time evidence base for analysis that may be used to determine cutting-edge heat-health relationships in Toronto in the future.

4.5.2 Heat-related Illness Mis-Diagnosis

The MPDS is designed to make quick decisions regarding the patient's needs when a call is made, often focusing less on assigning an accurate medical diagnosis. This rapid assessment can potentially lead to the over-turning of calls that were originally classified as 'heat exposure' to a different diagnosis and vice versa. In addition, this study utilizes a broader subset of MPDS codes that have been previously designated as possible HR health issues which do not specifically include the word 'heat' within their code. However, there is a strong likelihood that not all of the health issues within the subset of MPDS codes used were directly HR on a given day or within a given hour. This study, therefore, may have inherently

mis-represented or overestimated the total number of calls that are directly attributed to heat. Lower correlations among the heat stress metrics and the HR EMS ambulance response calls may have occurred as a result.

4.5.3 Heat-related EMS Caller Information Deficiency

Without additional data such as the socio-economic status, demographic information, and geographic origin of a caller, as well as the activities participated in prior to the call and whether the caller was inside or outside, it is difficult to explain why higher call ratios were observed in certain locations within the city of Toronto. Harlan and Ruddell (2011) and Reid et al. (2009) express the importance of possessing such additional data for indentification of the most vulnerable populations within a city since health burdens fall disproportionately on urban residents. For example, are those most at risk visiting tourists, engaged in physical activities, or living in poorer housing types with no air conditioning or in local hot spot areas? Although identifying such spatial risk factors in Toronto during the summer of 2015 was not a primary objective of this particular study, access to and analyses of these types of factors could prove beneficial to ensuring that EMS dispatch services are targeted to the most vulnerable populations beyond just the areas of escalated heat exposure as were pinpointed in this study. However, in many cases this caller information is not included in available medical dispatch data due to confidentiality constraints.

4.6 Conclusions

This study assessed the spatiotemporal relationships between five heat stress metrics and HR EMS ambulance response calls in Toronto, Canada during a large-scale sports event. The five heat metrics examined were T_{max}, T_{min}, the

humidex, the WBGT index, and the COMFA human EB model. Novel fine-scale meteorological data, from a within-city mesonet system of 53 weather stations, were used as input to calculate heat metric values on an hourly time scale for various locations across the GTA for July and August 2015. All EMS response calls and the respective call locations for the duration of this time period were utilized as well. EMS response call results were reported as 'calls per 100,000', a number that may be more useful for planners who can multiply the rates by the estimated population present and obtain a number of anticipated heat-related illness patients. This unique combination of fine-scale meteorological data with EMS call data was applied in three ways: 1) to determine the GTA's areas of escalated heat exposure, 2) to demonstrate the ability of various heat metrics and spatial exposure proxies to predict heat-related EMS response calls, and 3) to showcase the benefits of using outdoor EB modeling as a meaningful tool for heat stress forecasting at mass gathering events.

Results reveal an overall consensus among heat metrics that Hamilton, Ontario was the area of greatest escalated risk for HR illness within the GTA, that generally weak relationships existed between HR EMS response calls and the heat metrics, with the 'station-specific' proxy and the COMFA metric showing the strongest relationships, and that spectator and physically active athlete human EB variations during Games events were largely influenced by R_{abs} and M_{act} values. These results are significant because they emphasize the various potential benefits and products (e.g., heat vulnerability maps, public real-time local weather information) that can come from implementing such a mesonet monitoring network for both short-term and long-term purposes. The analysis performed in this study could provide even more detail if additional demographic, socio-economic, and situational data is acquired regarding the heat-related EMS response calls. These results can be

utilized by urban planners and EMS personnel to be aware of areas of high heat stress, thereby knowing the most crucial areas in which to implement corrective bioclimatic design and dispatch EMS resources to, respectively, on days of excessive heat.

BIBLIOGRAPHY

Ainsworth, B., et al., 2011: 2011 Compendium of Physical Activities: a second update of codes and MET values. *Medicine and Science in Sports and Exercise*, **43 (8)**, 1575–1581.

Alessandrini, E., S. Zauli Sajani, F. Scotto, R. Miglio, S. Marchesi, and P. Lauriola, 2011: Emergency ambulance dispatches and apparent temperature: A time series analysis in Emilia-Romagna, Italy. *Environmental Research*, **111 (8)**, 1192–1200, doi:10.1016/j.envres.2011.07.005, URL `http://dx.doi.org/10.1016/j.envres.2011.07.005`.

Anderson, B. G. and M. L. Bell, 2011: Heat waves in the United States: Mortality risk during heat waves and effect modification by heat wave characteristics in 43 U.S. communities. *Environmental Health Perspectives*, **119 (2)**, 210–218, doi:10.1289/ehp.1002313.

Anderson, J. and J. Usher, 2010: Mesonet Programs - Needs and Best Practices. Tech. rep.

Armstrong, L. E., D. J. Casa, M. Millard-Stafford, D. S. Moran, S. W. Pyne, and W. O. Roberts, 2007: Exertional heat illness during training and competition. *Medicine and Science in Sports and Exercise*, **39 (3)**, 556–572, doi:10.1249/MSS.0b013e31802fa199.

Bassil, K. L., D. C. Cole, R. Moineddin, A. M. Craig, W. Y. Wendy Lou, B. Schwartz, and E. Rea, 2009: Temporal and spatial variation of heat-related illness using 911 medical dispatch data. *Environmental Research*, **109 (5)**, 600–606, doi:10.1016/j.envres.2009.03.011, URL `http://dx.doi.org/10.1016/j.envres.2009.03.011`.

Bassil, K. L., D. C. Cole, R. Moineddin, E. Gournis, B. Schwartz, A. M. Craig, W. Y. W. Lou, and E. Rea, 2008: Development of a surveillance case definition for heat-related illness using 911 medical dispatch data. *Canadian Journal of Public Health*, **99 (4)**, 339–343.

Bernhard, M. C., S. T. Kent, M. E. Sloan, M. B. Evans, L. A. McClure, and J. M. Gohlke, 2015: Measuring personal heat exposure in an urban and rural environment. *Environmental Research*, **137**, 410–418, doi:10.1016/j.envres.2014.11.002.

Black, E., M. Blackburn, G. Harrison, B. Hoskins, and J. Methven, 2004: Factors contributing to the summer 2003 European heatwave. *Weather*, **59 (8)**, 217–223.

Blair, R., 2006: Meteorological Variations and their Impact on NO2 Concentrations in the Toronto-Hamilton Urban Air-Shed. Ph.D. thesis.

Blazejczyk, K., Y. Epstein, G. Jendritzky, H. Staiger, and B. Tinz, 2012: Comparison of UTCI to selected thermal indices. *International Journal of Biometeorology*, **56 (3)**, 515–535, doi:10.1007/s00484-011-0453-2.

Brotherhood, J. R., 2008: Heat stress and strain in exercise and sport. *Journal of science and medicine in sport / Sports Medicine Australia*, **11 (1)**, 6–19, doi:10.1016/j.jsams.2007.08.017, URL http://www.sciencedirect.com/science/article/pii/S1440244007002095.

Brown, R. and T. Gillespie, 1995: *Microclimate landscape design: Creating thermal comfort and energy efficiency*. New York: John Wiley & Sons.

Brown, R. D., 2011: Ameliorating the effects of climate change: Modifying microclimates through design. *Landscape and Urban Planning*, **100 (4)**, 372–374, doi:10.1016/j.landurbplan.2011.01.010, URL http://dx.doi.org/10.1016/j.landurbplan.2011.01.010.

Brown, R. D. and T. J. Gillespie, 1986: Estimating outdoor thermal comfort using a cylindrical radiation thermometer and an energy budget model. *International Journal of Biometeorology*, **30 (1)**, 43–52, doi:10.1007/BF02192058.

Brown, R. D., J. Vanos, N. Kenny, and S. Lenzholzer, 2015: Designing urban parks that ameliorate the effects of climate change. *Landscape and Urban Planning*, **138**, 118–131, doi:10.1016/j.landurbplan.2015.02.006, URL http://dx.doi.org/10.1016/j.landurbplan.2015.02.006.

Budd, G. M., 2008: Wet-bulb globe temperature (WBGT)-its history and its limitations. *Journal of Science and Medicine in Sport*, **11 (1)**, 20–32, doi:10.1016/j.jsams.2007.07.003.

Canadian Centre for Occupational Health and Safety, 2017: Hot Environments - Control Measures: OSH Answers. URL https://www.ccohs.ca/oshanswers/phys_agents/heat_control.html.

Casa, D. J., et al., 2015: National athletic trainers' association position statement: Exertional heat illnesses. *Journal of Athletic Training*, **50 (9)**, 986–1000, doi:10.4085/1062-6050-50.9.07.

CDC, 2015: Natural Disasters and Severe Weather. URL https://www.cdc.gov/disasters/extremeheat/heat_guide.html.

Cheng, J., Z. Xu, D. Zhao, M. Xie, H. Yang, L. Wen, K. Li, and H. Su, 2016: Impacts of temperature change on ambulance dispatches and seasonal effect modification. *International Journal of Biometeorology*, **60 (12)**, 1863–1871, doi:10.1007/s00484-016-1173-4, URL http://dx.doi.org/10.1007/s00484-016-1173-4.

D'Ambrosio Alfano, F. R., J. Malchaire, B. I. Palella, and G. Riccio, 2014: WBGT index revisited after 60 years of use. *Annals of Occupational Hygiene*, **58 (8)**, 955–970, doi:10.1093/annhyg/meu050.

Dolney, T. J. and S. C. Sheridan, 2006: The relationship between extreme heat and ambulance response calls for the city of Toronto, Ontario, Canada. *Environmental Research*, **101 (1)**, 94–103, doi:10.1016/j.envres.2005.08.008.

Eichner, E. R., 2002: SSE #86: Heat Stroke in Sports: Causes, Prevention and Treatment. *Sports Science Exchange 86*, **15 (3)**.

Environment Canada, 2016: Climate Change Science and Research. URL `http://www.ec.gc.ca/sc-cs/Default.asp?lang5Enn556010B41-1`.

Epstein, Y. and D. S. Moran, 2006: Thermal comfort and the heat stress indices. *Industrial health*, **44 (3)**, 388–398, doi:10.2486/indhealth.44.388.

Erell, E., D. Pearlmutter, and T. Williamson, 2012: *Urban microclimate: designing the spaces between buildings*. Routledge.

Fanger, P., 1972: *Thermal Comfort New York*.

Gehrels, H., et al., 2016: Designing green and blue infrastructure to support healthy urban living.

Giannakis, E., A. Bruggeman, D. Poulou, C. Zoumides, and M. Eliades, 2016: Linear parks along urban rivers: Perceptions of thermal comfort and climate change adaptation in Cyprus. *Sustainability (Switzerland)*, **8 (10)**, doi:10.3390/su8101023.

Gill, S. E., J. F. Handley, a. R. Ennos, and S. Pauleit, 2007: Adapting cities for climate change: The role of the green infrastructure. *Built Environment*, **33 (1)**, 115–133, doi:10.2148/benv.33.1.115.

Golden, J. S., D. Hartz, A. Brazel, G. Luber, and P. Phelan, 2008: A biometeorology study of climate and heat-related morbidity in Phoenix from 2001 to 2006. *International Journal of Biometeorology*, **52 (6)**, 471–480, doi:10.1007/s00484-007-0142-3.

Goodman, P. G., D. W. Dockery, and L. Clancy, 2004: Cause-specific mortality and the extended effects of particulate pollution and temperature exposure. *Environmental Health Perspectives*, **112 (2)**, 179–185, doi:10.1289/ehp.6451.

Graham, D. A., J. K. Vanos, N. A. Kenny, and R. D. Brown, 2016: The relationship between neighbourhood tree canopy cover and heat-related ambulance calls during extreme heat events in Toronto, Canada. *Urban Forestry and Urban Greening*, **20**, 180–186, doi:10.1016/j.ufug.2016.08.005, URL `http://dx.doi.org/10.1016/j.ufug.2016.08.005`.

Grundstein, A., J. A. Knox, J. Vanos, E. R. Cooper, and D. J. Casa, 2017: American football and fatal exertional heat stroke: a case study of Korey Stringer. 1–10 pp., doi:10.1007/s00484-017-1324-2.

Hajat, S. and T. Kosatky, 2010: Heat-related mortality: a review and exploration of heterogeneity. *Journal of epidemiology and community health*, **64 (9)**, 753–760, doi:10.1136/jech.2009.087999.

Hajat, S., et al., 2010: Heat-health warning systems: A comparison of the predictive capacity of different approaches to identifying dangerously hot days. *American Journal of Public Health*, **100 (6)**, 1137–1144, doi:10.2105/AJPH.2009.169748.

Hamilton Paramedic Service, 2017: Personal Communication with Hamilton Paramedic Service.

Hansen, A., P. Bi, M. Nitschke, D. Pisaniello, J. Newbury, and A. Kitson, 2011: Older persons and heat-susceptibility: the role of health promotion in a changing climate. *Health Promot J Austr*, **22**, S17–20., URL `http://www.ncbi.nlm.nih.gov/pubmed/22518914#`.

Hardin, A. W. and J. K. Vanos, 2017: The influence of surface type on the absorbed radiation by a human under hot, dry conditions. *International Journal of Biometeorology*, doi:10.1007/s00484-017-1357-6, URL `http://link.springer.com/10.1007/s00484-017-1357-6`.

Harlan, S. L., A. J. Brazel, L. Prashad, W. L. Stefanov, and L. Larsen, 2006: Neighborhood microclimates and vulnerability to heat stress. *Social Science and Medicine*, **63 (11)**, 2847–2863, doi:10.1016/j.socscimed.2006.07.030.

Harlan, S. L. and D. M. Ruddell, 2011: Climate change and health in cities: Impacts of heat and air pollution and potential co-benefits from mitigation and adaptation. *Current Opinion in Environmental Sustainability*, **3 (3)**, 126–134, doi:10.1016/j.cosust.2011.01.001.

Hartz, D. A., A. J. Brazel, and J. S. Golden, 2013: A comparative climate analysis of heat-related emergency 911 dispatches: Chicago, Illinois and Phoenix, Arizona USA 2003 to 2006. *International Journal of Biometeorology*, **57 (5)**, 669–678, doi:10.1007/s00484-012-0593-z.

Havenith, G. and D. Fiala, 2015: Thermal Indices and Thermophysiological Modeling for Heat Stress. *Comprehensive Physiology*, **6 (1)**, 255–302, doi:10.1002/cphy.c140051, URL `http://www.ncbi.nlm.nih.gov/pubmed/26756633`.

Havenith, G., et al., 2012: The UTCI-clothing model. *International Journal of Biometeorology*, **56 (3)**, 461–470, doi:10.1007/s00484-011-0451-4.

Helbing, D. and A. Johansson, 2013: Pedestrian, Crowd, and Evacuation Dynamics. *Encyclopedia of Complexity and Systems Science*, **16 (4)**, 6476–6495, doi:10.1007/978-3-642-04504-2, URL `http://www.springerlink.com/index/10.1007/978-3-642-04504-2`, `arXiv:1309.1609v1`.

Hondula, D. M., R. E. Davis, M. J. Leisten, M. V. Saha, L. M. Veazey, and C. R. Wegner, 2012: Fine-scale spatial variability of heat-related mortality in Philadelphia County, USA, from 1983-2008: a case-series analysis. *Environmental Health: A Global Access Science Source*, **11 (1)**, 1–11, doi:10.1186/1476-069x-11-16.

Hoppe, P., 1999: The physiological equivalent temperature - a universal index for the biometeorological assessment of the thermal environment. *International journal of biometeorology*, **43 (2)**, 71–75, doi:10.1007/s004840050118.

ISO 9920, 2007: Ergonomics of the thermal environment - Estimation of thermal insulation and water vapour resistance of a clothing ensemble. *International Organization for Standardization*.

Jendritzky, G., R. de Dear, and G. Havenith, 2012: UTCI-Why another thermal index? *International Journal of Biometeorology*, **56 (3)**, 421–428, doi:10.1007/s00484-011-0513-7.

Jendritzky, G. and B. Tinz, 2009: The thermal environment of the human being on the global scale. *Global Health Action 2*, **1**, 1–13, doi:10.3402/gha.v2i0.2005.

Jenerette, G. D., et al., 2016: Micro-scale urban surface temperatures are related to land-cover features and residential heat related health impacts in Phoenix, AZ USA. *Landscape Ecology*, **31 (4)**, 745–760, doi:10.1007/s10980-015-0284-3, URL `"http://dx.doi.org/10.1007/s10980-015-0284-3`.

Johansson, E., S. Thorsson, R. Emmanuel, and E. Krüger, 2014: Instruments and methods in outdoor thermal comfort studiesThe need for standardization. *Urban Climate*, **10**, 346–366.

Johnson, D. P., A. Stanforth, V. Lulla, and G. Luber, 2012: Developing an applied extreme heat vulnerability index utilizing socioeconomic and environmental data. *Applied Geography*, **35 (1-2)**, 23–31, doi:10.1016/j.apgeog.2012.04.006, URL `http://dx.doi.org/10.1016/j.apgeog.2012.04.006`.

Kalkstein, L. S., 2000: Saving lives during extreme weather in summer: Interventions from local health agencies and doctors can reduce mortality. *British Medical Journal*, **321 (7262)**, 650.

Kalkstein, L. S. and R. E. Davis, 1989: Weather and human mortality: an evaluation of demographic and interregional responses in the United States. *Annals of the Association of American Geographers*, **79 (1)**, 44–64.

Kántor, N., A. Kovács, and T. P. Lin, 2014: Looking for simple correction functions between the mean radiant temperature from the standard black globe and the six-directional techniques in Taiwan. *Theoretical and Applied Climatology*, **121 (1-2)**, 99–111, doi:10.1007/s00704-014-1211-2.

Kántor, N. and J. Unger, 2011: The most problematic variable in the course of human-biometeorological comfort assessment the mean radiant temperature. *Open Geosciences*, **3 (1)**, 90–100, doi:10.2478/s13533-011-0010-x.

Kenny, N. A., J. S. Warland, R. D. Brown, and T. G. Gillespie, 2008: Estimating the radiation absorbed by a human. *International Journal of Biometeorology*, **52 (6)**, 491–503, doi:10.1007/s00484-008-0145-8.

Kenny, N. A., J. S. Warland, R. D. Brown, and T. G. Gillespie, 2009a: Part A: Assessing the performance of the comfa outdoor thermal comfort model on subjects performing physical activity. *International Journal of Biometeorology*, **53 (5)**, 415–428, doi:10.1007/s00484-009-0226-3.

Kenny, N. A., J. S. Warland, R. D. Brown, and T. G. Gillespie, 2009b: Part B: Revisions to the COMFA outdoor thermal comfort model for application to subjects performing physical activity. *International Journal of Biometeorology*, **53 (5)**, 429–441, doi:10.1007/s00484-009-0227-2.

Kinney, P. L., M. S. O'Neill, M. L. Bell, and J. Schwartz, 2008: Approaches for estimating effects of climate change on heat-related deaths: challenges and opportunities. *Environmental Science and Policy*, **11 (1)**, 87–96, doi:10.1016/j.envsci.2007.08.001.

Klysik, K. and K. Fortuniak, 1999: Temporal and spatial characteristics of the urban heat island of Lodz, Poland. *Atmospheric Environment*, **33 (24-25)**, 3885–3895, doi:doi:10.1016/S1352-2310(99)00131-4, URL `<Go to ISI>://000082257400003`.

Kuras, E., et al., 2017: Opportunities and Challenges for Personal Heat Exposure Research. *Environmental Health Perspectives*.

Kuras, E. R., D. M. Hondula, and J. Brown-Saracino, 2015: Heterogeneity in individually experienced temperatures (IETs) within an urban neighborhood: insights from a new approach to measuring heat exposure. *International Journal of Biometeorology*, **59 (10)**, 1363–1372, doi:10.1007/s00484-014-0946-x.

Larsen, T., S. Kumar, K. Grimmer, A. Potter, T. Farquharson, and P. Sharpe, 2007: A systematic review of guidelines for the prevention of heat illness in

community-based sports participants and officials. *Journal of Science and Medicine in Sport*, **10 (1)**, 11–26, doi:10.1016/j.jsams.2006.07.008.

Lemmen, D. S., et al., 2008: *From Impacts to adaptation:Canada in a Changing Climate 2007*. 448 pp.

Lin, T.-P. and A. Matzarakis, 2011: Tourism climate information based on human thermal perception in Taiwan and Eastern China. *Tourism Management*, **32 (3)**, 492–500, doi:10.1016/j.tourman.2010.03.017, URL `http://dx.doi.org/10.1016/j.tourman.2010.03.017`.

Lu, S., H. Xia, S. Wei, K. Fang, and Y. Qi, 2016: Analysis of the differences in thermal comfort between locals and tourists and genders in semi-open spaces under natural ventilation on a tropical island. *Energy and Buildings*, **129**, 264–273, doi:10.1016/j.enbuild.2016.08.002, URL `http://dx.doi.org/10.1016/j.enbuild.2016.08.002`.

Luber, G. and M. McGeehin, 2008: Climate Change and Extreme Heat Events. *American Journal of Preventive Medicine*, **35 (5)**, doi:10.1016/j.amepre.2008.08.021.

Maloney, S. K. and C. F. Forbes, 2011: What effect will a few degrees of climate change have on human heat balance? Implications for human activity. *International Journal of Biometeorology*, **55 (2)**, 147–160, doi:10.1007/s00484-010-0320-6.

Matzarakis, A., 2006: Weather- and climate-related information for tourism. *Tourism and Hospitality Planning & Development*, **3 (2)**, 99–115, doi:10.1080/14790530600938279.

Matzarakis, A. and D. Frohlich, 2014: Sport events and climate for visitors - the case of FIFA World Cup in Qatar 2022. *International Journal of Biometeorology*, **59 (4)**, 481–486, doi:10.1007/s00484-014-0886-5.

McGeehin, M. and M. Mirabelli, 2001: The potential impacts of climate variability and change on temperature-related morbidity and mortality in the United States. *Environmental health perspectives*, **109 Suppl (May)**, 185–9, doi:10.2307/3435008.

McGregor, G. and J. Vanos, in review: Heat: A Primer for Public Health Researcers. *Submitted to Public Health*.

Meehl, G. A., 2004: More Intense, More Frequent, and Longer Lasting Heat Waves in the 21st Century. *Science*, **305 (5686)**, 994–997, doi:10.1126/science.1098704, URL `http://www.sciencemag.org/cgi/doi/10.1126/science.1098704`.

Meyer, S. J. and K. G. Hubbard, 1992: Nonfederal Automated Weather Stations and Networks in the United States and Canada: A Preliminary Survey. 449–457 pp., doi:10.1175/1520-0477(1992)073¡0449:NAWSAN¿2.0.CO;2.

Milsten, A. M., B. J. Maguire, R. a. Bissell, and K. G. Seaman, 2002: Mass-gathering medical care: a review of the literature. *Prehospital and disaster medicine*, **17 (03)**, 151–162, doi:10.1017/S1049023X00000388.

Milsten, A. M., K. G. Seaman, P. Liu, R. a. Bissell, and B. J. Maguire, 2004: Variables influencing medical usage rates, injury patterns, and levels of care for mass gatherings. *Prehospital and Disaster Medicine*, **18 (4)**, 334–46, doi:10.1017/S1049023X00001291, URL `http://www.ncbi.nlm.nih.gov/pubmed/15310046`.

Miralles, D. G., A. J. Teuling, C. C. van Heerwaarden, and J. Vilà-Guerau de Arellano, 2014: Mega-heatwave temperatures due to combined soil desiccation and atmospheric heat accumulation. *Nature Geoscience*, **7 (5)**, 345–349, doi:10.1038/ngeo2141, URL `http://www.nature.com/doifinder/10.1038/ngeo2141`.

Monteith, J. L. and M. H. Unsworth, 1990: Principles of environmental physics, 2nd Edition. *Edward Arnold, London*, 197, doi:10.1016/B978-0-12-386910-4.00026-3.

Muller, C. L., L. Chapman, C. S. B. Grimmond, D. T. Young, and X. Cai, 2013: Sensors and the city: A review of urban meteorological networks. *International Journal of Climatology*, **33 (7)**, 1585–1600, doi:10.1002/joc.3678.

Nadel, E., C. Wenger, M. Roberts, J. Stolwijk, and E. Cafarelli, 1977: Physiological defenses against hyperthermia of exercise. *Annals of the New York Academy of Sciences*, **301 (1)**, 98–109.

Ng, C. F. S., K. Ueda, M. Ono, H. Nitta, and A. Takami, 2014: Characterizing the effect of summer temperature on heatstroke-related emergency ambulance dispatches in the Kanto area of Japan. *International Journal of Biometeorology*, **58 (5)**, 941–948, doi:10.1007/s00484-013-0677-4.

Ng, E., 2012: Towards planning and practical understanding of the need for meteorological and climatic information in the design of high-density cities: A case-based study of Hong Kong. *International Journal of Climatology*, **32 (4)**, 582–598, doi:10.1002/joc.2292.

Niu, Y., R. Chen, C. Liu, P. Ran, A. Chen, X. Chen, and H. Kan, 2016: The association between ambient temperature and out-of-hospital cardiac arrest in Guangzhou, China. *Science of The Total Environment*, **572**, 114–118, doi:10.1016/j.scitotenv.2016.07.205, URL `http://linkinghub.elsevier.com/retrieve/pii/S004896971631659X`.

Oke, T. R., 1987: *Boundary layer climates, Second edition.* 435 pp., doi:10.1017/CBO9781107415324.004, arXiv:1011.1669v3.

Oke, T. R. and F. Hannell, 1970: The form of the urban heat island in Hamilton, Canada. *WMO Technical Note*, **108**, 113–126.

Oleson, K. W., A. Monaghan, O. Wilhelmi, M. Barlage, N. Brunsell, J. Feddema, L. Hu, and D. F. Steinhoff, 2015: Interactions between urbanization, heat stress, and climate change. *Climatic Change*, **129 (3-4)**, 525–541, doi:10.1007/s10584-013-0936-8.

Peel, B., B. L. Finlayson, and T. A. McMahon, 2007: Updated world map of the Koppen-Geiger climate classication.pdf. *Hydrology and Earth System Sciences*, **11 (2001)**, 1633–1644, doi:10.5194/hess-11-1633-2007, URL http://www.hydrol-earth-syst-sci.net/11/1633/2007/hess-11-1633-2007.pdf.

Penney, J., 2008: Climate change adaptation in the city of Toronto: lessons for Great Lakes Communities. *Clean Air Partnership*.

Perini, K. and A. Magliocco, 2014: Effects of vegetation, urban density, building height, and atmospheric conditions on local temperatures and thermal comfort. *Urban Forestry and Urban Greening*, **13 (3)**, 495–506, doi:10.1016/j.ufug.2014.03.003, URL http://dx.doi.org/10.1016/j.ufug.2014.03.003.

Perron, A. D., W. J. Brady, C. B. Custalow, and D. M. Johnson, 2005: ASSOCIATION OF HEAT INDEX andPATIENT VOLUME AT A MASS GATHERING EVENT. *Prehospital Emergency Care*, **9 (1)**, 49–52, doi:10.1080/10903120590891976, URL http://www.tandfonline.com/doi/full/10.1080/10903120590891976.

Psikuta, A., et al., 2012: Validation of the Fiala multi-node thermophysiological model for UTCI application. *International Journal of Biometeorology*, **56 (3)**, 443–460, doi:10.1007/s00484-011-0450-5.

Reid, C., M. O'Neill, C. Gronlund, S. Brines, D. Brown, A. Diez-Roux, and J. Schwartz, 2009: Mapping Community Determinants of Heat Vulnerability. *Environmental health perspectives*, **117 (11)**, 1730–1736, doi:10.1289/ehp.0900683.

Resch, B., M. Mittleboeck, S. Lipson, M. Welsh, J. Bers, R. Britter, C. Ratti, and T. Blaschke, 2011: Integrated Urban Sensing: A Geo-sensor Network for Public Health Monitoring and Beyond. *International Journal of Geographical Information Science*, URL http://dspace.mit.edu/handle/1721.1/64636.

Rinner, C. and M. Hussain, 2011: Toronto's urban heat island-exploring the relationship between land use and surface temperature. *Remote Sensing*, **3 (6)**, 1251–1265, doi:10.3390/rs3061251.

Salata, F., I. Golasi, A. D. L. Vollaro, and R. D. L. Vollaro, 2015: How high albedo and traditional buildings' materials and vegetation affect the quality of urban microclimate. A case study. *Energy and Buildings*, **99**, 32–49, doi:10.1016/j.enbuild.2015.04.010, URL `http://dx.doi.org/10.1016/j.enbuild.2015.04.010`.

Scott, D. and C. Lemieux, 2010: Weather and climate information for tourism. *Procedia Environmental Sciences*, **1 (1)**, 146–183, doi:10.1016/j.proenv.2010.09.011, URL `http://dx.doi.org/10.1016/j.proenv.2010.09.011`.

Scutchfield, F. and C. Keck, 2003: *Principles of public health practice*. Cengage Learning.

Sheridan, S. C., A. J. Kalkstein, and L. S. Kalkstein, 2009: Trends in heat-related mortality in the United States, 1975-2004. *Natural Hazards*, **50 (1)**, 145–160, doi:10.1007/s11069-008-9327-2.

Sheridan, S. C. and L. S. Kalkstein, 2004: Progress in heat watch-warning system technology. *Bulletin of the American Meteorological Society*, **85 (12)**, 1931–1941, doi:10.1175/BAMS-85-12-1931.

Sills, D., 2017: Personal communication with David Sills (Environment Canada).

Smoyer-Tomic, K. E. and D. G. C. Rainham, 2001: Beating the heat: Development and evaluation of a Canadian hot weather health-response plan. *Environmental Health Perspectives*, **109 (12)**, 1241–1248, doi:10.1289/ehp.011091241.

Sofotasiou, P., B. R. Hughes, and J. K. Calautit, 2015: Qatar 2022: Facing the FIFA World Cup climatic and legacy challenges. *Sustainable Cities and Society*, **14 (1)**, 16–30, doi:10.1016/j.scs.2014.07.007.

Solis, P., J. K. Vanos, and R. Forbis, 2016: The Decision-Making/Accountability Spatial Incongruence Problem for research linking environmental science and policy. *Geographical Review*, 1–25, doi:10.1111/gere.12240, URL `http://doi.wiley.com/10.1111/gere.12240`.

Steffen, R., A. Bouchama, A. Johansson, J. Dvorak, N. Isla, C. Smallwood, and Z. a. Memish, 2012: Non-communicable health risks during mass gatherings. *The Lancet Infectious Diseases*, **12 (2)**, 142–149, doi:10.1016/S1473-3099(11)70293-6.

Stewart, I. D. and T. R. Oke, 2012: Local climate zones for urban temperature studies. *Bulletin of the American Meteorological Society*, **93 (12)**, 1879–1900, doi:10.1175/BAMS-D-11-00019.1, `arXiv:1011.1669v3`.

Strath, S., A. Swartz, D. Bassett, W. OBrien, G. King, and B. Ainsworth, 2000: Evaluation of heart rate as a method for assessing moderate intensity physical activity. *Medicine and Science in Sports and Exercise*, **32**, 465–470.

Taleghani, M., L. Kleerekoper, M. Tenpierik, and A. Van Den Dobbelsteen, 2015: Outdoor thermal comfort within five different urban forms in the Netherlands. *Building and Environment*, **83**, 65–78, doi:10.1016/j.buildenv.2014.03.014, URL `http://dx.doi.org/10.1016/j.buildenv.2014.03.014`.

Tamerius, J. D., E. K. Wise, C. K. Uejio, A. L. McCoy, and A. C. Comrie, 2007: Climate and human health: Synthesizing environmental complexity and uncertainty. *Stochastic Environmental Research and Risk Assessment*, **21 (5)**, 601–613, doi:10.1007/s00477-007-0142-1.

Thorsson, S., F. Lindberg, I. Eliasson, and B. Holmer, 2007: Different methods for estimating the mean radiant temperature in an outdoor urban setting. *International Journal of Climatology*, Vol. 27, 1983–1993, doi:10.1002/joc.1537, `joc.1492`.

Tsunematsu, N., H. Yokoyama, T. Honjo, A. Ichihashi, H. Ando, and N. Shigyo, 2016: Relationship between land use variations and spatiotemporal changes in amounts of thermal infrared energy emitted from urban surfaces in downtown Tokyo on hot summer days. *Urban Climate*, **17**, 67–79, doi:10.1016/j.uclim.2016.03.002, URL `http://dx.doi.org/10.1016/j.uclim.2016.03.002`.

Uejio, C. K., O. V. Wilhelmi, J. S. Golden, D. M. Mills, S. P. Gulino, and J. P. Samenow, 2011: Intra-urban societal vulnerability to extreme heat: The role of heat exposure and the built environment, socioeconomics, and neighborhood stability. *Health and Place*, **17 (2)**, 498–507, doi:10.1016/j.healthplace.2010.12.005, URL `http://dx.doi.org/10.1016/j.healthplace.2010.12.005`.

United Nations Department of Economic and Social Affairs Population Division, 2014: World Urbanization Prospects: The 2014 Revision, Highlights. United Nations.

Vanos, J., A. Herdt, and M. Lochbaum, in review: Effects of Physical Activity and Shade on the Heat Balance and Thermal Perceptions of Children in a Playground Microclimate. *Submitted to Building and Environment*.

Vanos, J. K., A. Middel, G. R. McKercher, E. R. Kuras, and B. L. Ruddell, 2016: Hot playgrounds and children's health: A multiscale analysis of surface temperatures in Arizona, USA. *Landscape and Urban Planning*, **146**, 29–42, doi:10.1016/j.landurbplan.2015.10.007, URL `http://dx.doi.org/10.1016/j.landurbplan.2015.10.007`.

Vanos, J. K., J. S. Warland, T. J. Gillespie, and N. A. Kenny, 2012a: Improved predictive ability of climate-human-behaviour interactions with modifications to the COMFA outdoor energy budget model. *International Journal of Biometeorology*, **56 (6)**, 1065–1074, doi:10.1007/s00484-012-0522-1.

Vanos, J. K., J. S. Warland, T. J. Gillespie, and N. A. Kenny, 2012b: Thermal comfort modelling of body temperature and psychological variations of a human exercising in an outdoor environment. *International Journal of Biometeorology*, **56 (1)**, 21–32, doi:10.1007/s00484-010-0393-2, `ISBN 0 86776729 4`.

Vanos, J. K., J. S. Warland, T. J. Gillespie, G. A. Slater, R. D. Brown, and N. A. Kenny, 2012c: Human energy budget modeling in urban parks in toronto and applications to emergency heat stress preparedness. *Journal of Applied Meteorology and Climatology*, **51 (9)**, 1639–1653, doi:10.1175/JAMC-D-11-0245.1.

Wang, Y., U. Berardi, and H. Akbari, 2016: Comparing the effects of urban heat island mitigation strategies for Toronto, Canada. *Energy and Buildings*, **114**, 2–19, doi:10.1016/j.enbuild.2015.06.046, URL `http://dx.doi.org/10.1016/j.enbuild.2015.06.046`.

Wetterhall, S. F., D. M. Coulombier, J. M. Herndon, S. Zaza, and J. D. Cantwell, 1998: Medical care delivery at the 1996 Olympic Games. *The Journal of the American Medical Association*, **279 (18)**, 1463–1468.

White-Newsome, J. L., S. J. Brines, D. G. Brown, J. Timothy Dvonch, C. J. Gronlund, K. Zhang, E. M. Oswald, and M. S. O'Neill, 2013: Validating satellite-derived land surface temperature with in situ measurements: A public health perspective. *Environmental Health Perspectives*, **121 (8)**, 925–931, doi:10.1289/ehp.1206176.

Yaghoobian, N., J. Kleissl, and E. S. Krayenhoff, 2010: Modeling the thermal effects of artificial turf on the urban environment. *Journal of Applied Meteorology and Climatology*, **49 (3)**, 332–345, doi:10.1175/2009JAMC2198.1.

Yardley, J., R. J. Sigal, and G. P. Kenny, 2011: Heat health planning: The importance of social and community factors. *Global Environmental Change*, **21 (2)**, 670–679, doi:10.1016/j.gloenvcha.2010.11.010, URL `http://dx.doi.org/10.1016/j.gloenvcha.2010.11.010`.

Zhang, K., Y. Li, J. D. Schwartz, and M. S. O'Neill, 2014: What weather variables are important in predicting heat-related mortality? A new application of statistical learning methods. *Environmental Research*, **132**, 350–359, doi:10.1016/j.envres.2014.04.004, URL http://dx.doi.org/10.1016/j.envres.2014.04.004.

Zhang, K., R. B. Rood, G. Michailidis, E. M. Oswald, J. D. Schwartz, A. Zanobetti, K. L. Ebi, and M. S. O'Neill, 2012: Comparing exposure metrics for classifying 'dangerous heat' in heat wave and health warning systems. *Environment International*, **46**, 23–29, doi:10.1016/j.envint.2012.05.001, URL http://dx.doi.org/10.1016/j.envint.2012.05.001.

APPENDIX A

Table A.1: Mesonet weather station locations, LCZs, and surface covers.

STN NUMBER	STN NAME	LAT	LONG	LCZ	SFC COVER
6116200	UDORA (STRONG)	44.250°N	-79.200°W	C - Bush, scrub	Grass
6116201	HARDWOOD MOUNTAIN BIKE	44.517°N	-79.583°W	B - Scattered trees	Grass
6136285	ATMOS FENWICK	43.050°N	-79.367°W	9B - Sparsely built with scattered trees	Grass
6136290	ROYAL CANADIAN HENLEY	43.191°N	-79.267°W	9F - Sparsely built with sand	Sand/Gravel
6136300	VINELAND (STONEY RIDGE)	43.150°N	-79.383°W	9B - Sparsely built with scattered trees	Grass/Gravel
6136303	WAINFLEET (SKYDIVE)	42.883°N	-79.350°W	D - Low plants	Grass
6136305	WELLAND FLATWATER CNTR	42.967°N	-79.250°W	CG - Bush, scrub, and water	Membrane
6136308	WINONA (VINE ESTATES)	43.217°N	-79.683°W	6E - Open low-rise with bare rock	Gravel
6140942	BRANTFORD AIRPORT	43.133°N	-80.333°W	N/A	N/A
6153170	HALTON HILLS	43.600°N	-80.050°W	9CD - Sparsely built with low plants	Grass
6156130	ATMOS BRAMPTON	43.783°N	-79.767°W	D - Low plants	Grass
6156131	ATMOS CAMPBELLVILLE	43.450°N	-80.017°W	BD - Scattered trees and low plants	Grass
6156132	ATMOS CLAREMONT	43.933°N	-79.083°W	9B - Sparsely built with scattered trees	Grass
6156133	ATMOS ERIN	43.833°N	-80.117°W	B - Scattered tress	Grass
6156134	ATMOS HAMILTON	43.200°N	-79.833°W	D - Low plants	Grass
6156135	ATMOS MISSISSAUGA	43.533°N	-79.650°W	5B - Open midrise with scattered trees	Grass
6156136	ATMOS NORTH YORK	43.750°N	-79.317°W	4 - Open high-rise	Gravel
6156137	ATMOS NORVAL	43.617°N	-79.833°W	D - Low plants	Grass
6156138	ATMOS VAUGHAN	43.867°N	-79.533°W	6B - Open low-rise with scattered trees	Grass
6156150	AJAX COMMUNITY CNTR	43.867°N	-79.033°W	5 - Open midrise	Gravel
6156152	AJAX (PAO TAU)	43.900°N	-79.050°W	D - Low plants	Grass
6156153	AJAX (VILLAGE CHRYSLER)	43.833°N	-79.033°W	3E - Compact low-rise with bare rock	Gravel
6156154	AJAX (WINTERMERE SOD)	43.900°N	-79.033°W	D - Low plants	Grass
6156155	AJAX (WATER SUPPLY)	43.817°N	-79.000°W	5 - Open midrise	Stone
6156156	CALEDON EQUESTRIAN PARK	43.967°N	-79.833°W	9C - Sparsely built with bush and scrub	Grass
6156157	DUFFERIN / ST. CLAIR CIBC	43.867°N	-79.033°W	3 - Compact low-rise	Shingles
6156158	CLAREMONT (SILO FARM)	44.000°N	-79.100°W	D - Low plants	Grass
6156159	TORONTO TRAP AND SKEET	44.183°N	-79.667°W	9B - Sparsely built with scattered trees	Stone/Tar
6156160	CONCORD (RYDER)	43.817°N	-79.517°W	8 - Large low-rise	Gravel
6156161	DOWNSVIEW PARK	43.750°N	-79.483°W	8 - Large low-rise	Gravel
6156162	KING CITY	43.967°N	-79.567°W	9 - Sparsely built	Grass
6156164	HERSHEY CNTR	43.633°N	-79.650°W	5B - Open midrise with scattered trees	Membrane
6156165	MARKHAM (NORTH TOYOTA)	43.817°N	-79.350°W	8- Large low-rise	Gravel
6156166	BOUSFIELD FARMS	43.483°N	-79.900°W	9C - Sparsely built with bush and scrub	Grass
6156168	TORONTO (NORTH YORK)	43.717°N	-79.467°W	2 - Compact midrise	Gravel
6156169	GENERAL MOTORS CNTR	43.897°N	-78.867°W	2 - Compact midrise	Membrane
6156170	DOWNSVIEW	43.783°N	-79.467°W	5 - Open midrise	Grass
6156171	ROYAL CANADIAN YACHT CLUB	43.633°N	-79.350°W	5EG - Open midrise with bare rock and water	Grass
6156172	SCARBOROUGH (TORONTO HUNT)	43.683°N	-79.267°W	9D - Sparsely built with low plants	Grass
6156174	STONEY CREEK CARDINAL	43.217°N	-79.750°W	8 - Large low-rise	Gravel
6156175	MATTAMY ATHLETIC CNTR	43.667°N	-79.383°W	1 - Compact high-rise	Membrane
6156177	TORONTO (HYUNDAI)	43.699°N	-79.450°W	2 - Compact midrise	Gravel
6156179	U OF T SCARBOROUGH TENNIS	43.783°N	-79.183°W	9CE - Sparsely built with bush and bare rock	Stone
6156180	MONOPOLY PROPERTY	43.850°N	-79.300°W	5CE - Open midrise with bush and and bare rock	Tar
6156181	UXBRIDGE (LEE ACRES)	44.167°N	-79.217°W	C - Bush and scrub	Grass
6156182	UXBRIDGE (TARIS)	44.050°N	-79.117°W	9 - Sparsely built	Stone
6156183	YORK UNIVERSITY	43.783°N	-79.517°W	5 - Open midrise	Grass
6156184	WHITBY ABILITIES CNTR	43.867°N	-78.950°W	6 - Open low-rise	Concrete
6156186	ANGUS GLEN GOLF CLUB	43.902°N	-79.317°W	D - Low plants	Grass
6156187	HAMILTON SOCCER CNTR	43.250°N	-79.833°W	6 - Open low-rise	Mulch
6157000	MONO CNTR	43.033°N	-80.017°W	C - Bush and scrub	Grass/Dirt
6159123	UXBRIDGE WEST	44.100°N	-79.167°W	N/A	N/A
6166400	BLAIRHAMPTON GOLF CLUB	44.996°N	-78.667°W	D - Low plants	Grass

APPENDIX B

Table B.1: Station-specific seasonal summer heat stress metric values.

STN NUMBER	T_{max} (°C)	Humidex (°C)	WBGT (°C)	COMFA (Wm^{-2})
6116200	25.2	28.1	21.4	226.6
6116201	23.9	27.7	21.5	286.2
6136285	N/A	31.0	23.4	315.7
6136290	25.6	30.1	22.5	317.3
6136300	26.4	29.9	22.6	298.5
6136303	24.5	28.7	21.5	307.2
6136305	25.4	30.1	22.3	330.4
6136308	26.7	29.8	22.4	328.8
6140942	26.1	29.4	N/A	N/A
6153170	24.1	27.1	20.9	328.5
6156130	N/A	29.7	22.5	357.3
6156131	N/A	30.0	22.2	279.0
6156132	N/A	29.8	22.5	296.9
6156133	N/A	27.9	21.7	319.2
6156134	N/A	30.4	22.7	362.6
6156135	N/A	30.3	22.7	354.8
6156136	N/A	29.4	22.3	321.5
6156137	N/A	30.0	22.6	350.6
6156138	N/A	29.8	22.6	339.8
6156150	25.5	28.3	21.6	318.1
6156152	25.6	28.9	22.0	286.7
6156153	24.9	27.5	20.9	328.0
6156154	24.9	28.0	21.6	340.8
6156155	23.3	27.1	21.1	315.4
6156156	25.2	27.8	20.9	275.5
6156157	26.6	29.1	21.8	307.6
6156158	24.7	27.8	21.6	292.6
6156159	25.1	29.2	22.6	320.7
6156160	26.5	28.8	21.6	326.9
6156161	26.3	28.8	21.4	313.1
6156162	24.8	27.6	21.3	282.9
6156164	26.2	29.8	22.6	391.5
6156165	26.5	28.7	21.8	353.6
6156166	25.5	29.9	22.5	333.3
6156168	26.0	28.4	21.4	333.6
6156169	26.2	29.7	23.1	327.4
6156170	26.7	29.8	22.7	280.2
6156171	24.6	28.6	21.8	316.2
6156172	23.7	27.2	21.2	304.7
6156174	26.7	29.5	22.0	352.3
6156175	26.1	29.7	23.2	299.2
6156177	25.9	28.3	21.5	338.2
6156179	25.4	29.0	22.5	298.6
6156180	26.3	30.1	22.7	317.6
6156181	25.0	28.2	21.7	297.7
6156182	24.3	27.0	20.9	265.1
6156183	26.4	29.2	22.1	295.6
6156184	24.8	28.9	22.1	349.3
6156186	25.4	29.2	22.2	334.2
6156187	27.2	30.9	23.3	328.7
6157000	24.0	26.7	N/A	N/A
6159123	24.4	27.1	N/A	N/A
6166400	24.1	27.5	22.1	285.5

APPENDIX C

Figure C.1. The EBs (red line) and corresponding EB streams (M (purple line), R_{abs} (yellow line), C (blue line), E (orange line), and L_{emit} (green line)) for A) the men's bronze medal match, B) the women's gold medal match, and C) the men's gold medal match.

APPENDIX D

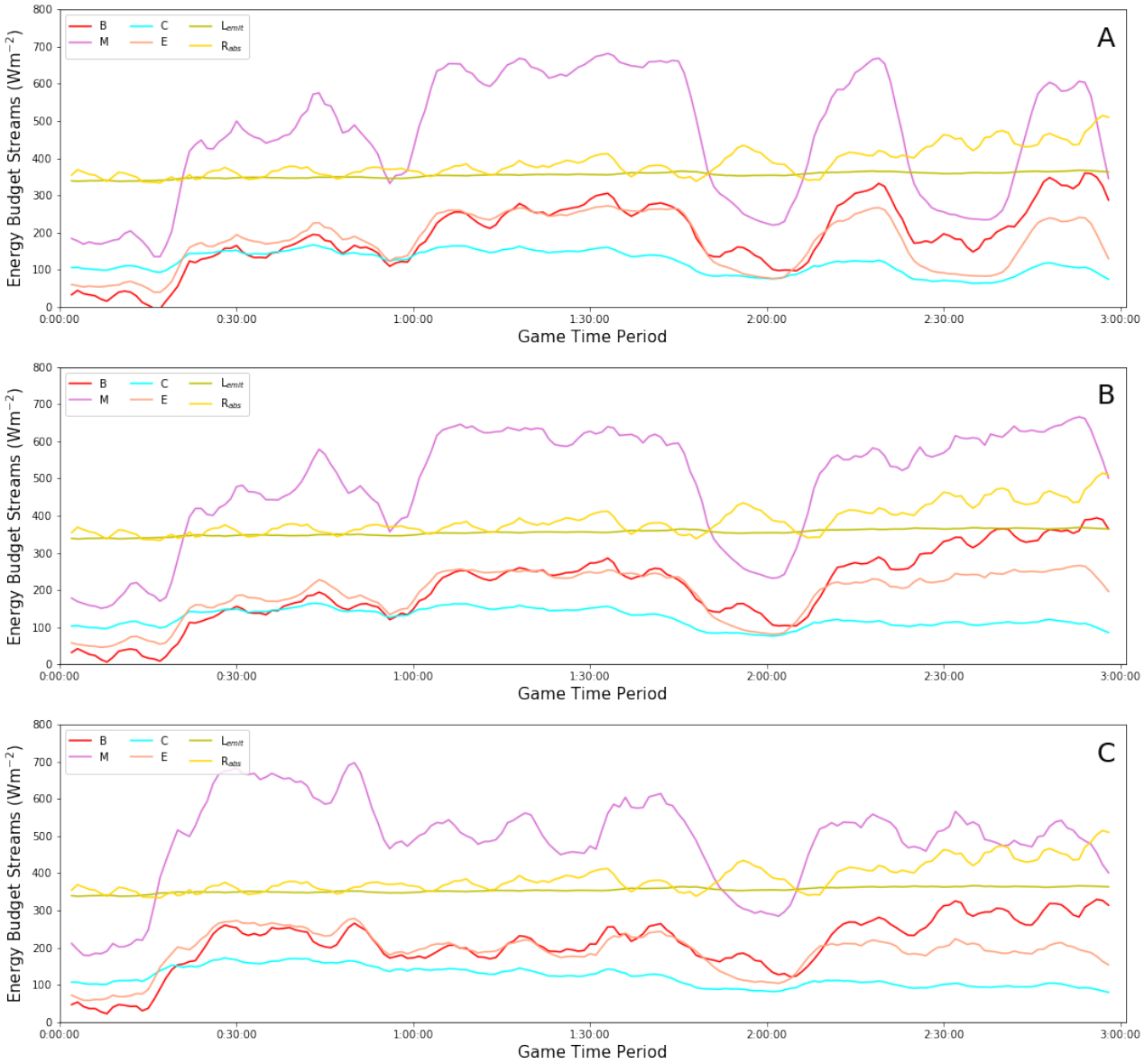

Figure D.1. The EBs (red line) and corresponding EB streams (M (purple line), R_{abs} (yellow line), C (blue line), E (orange line), and L_{emit} (green line)) for A) the midfielder B) the defender, and C) the goalie for the men's bronze medal match.

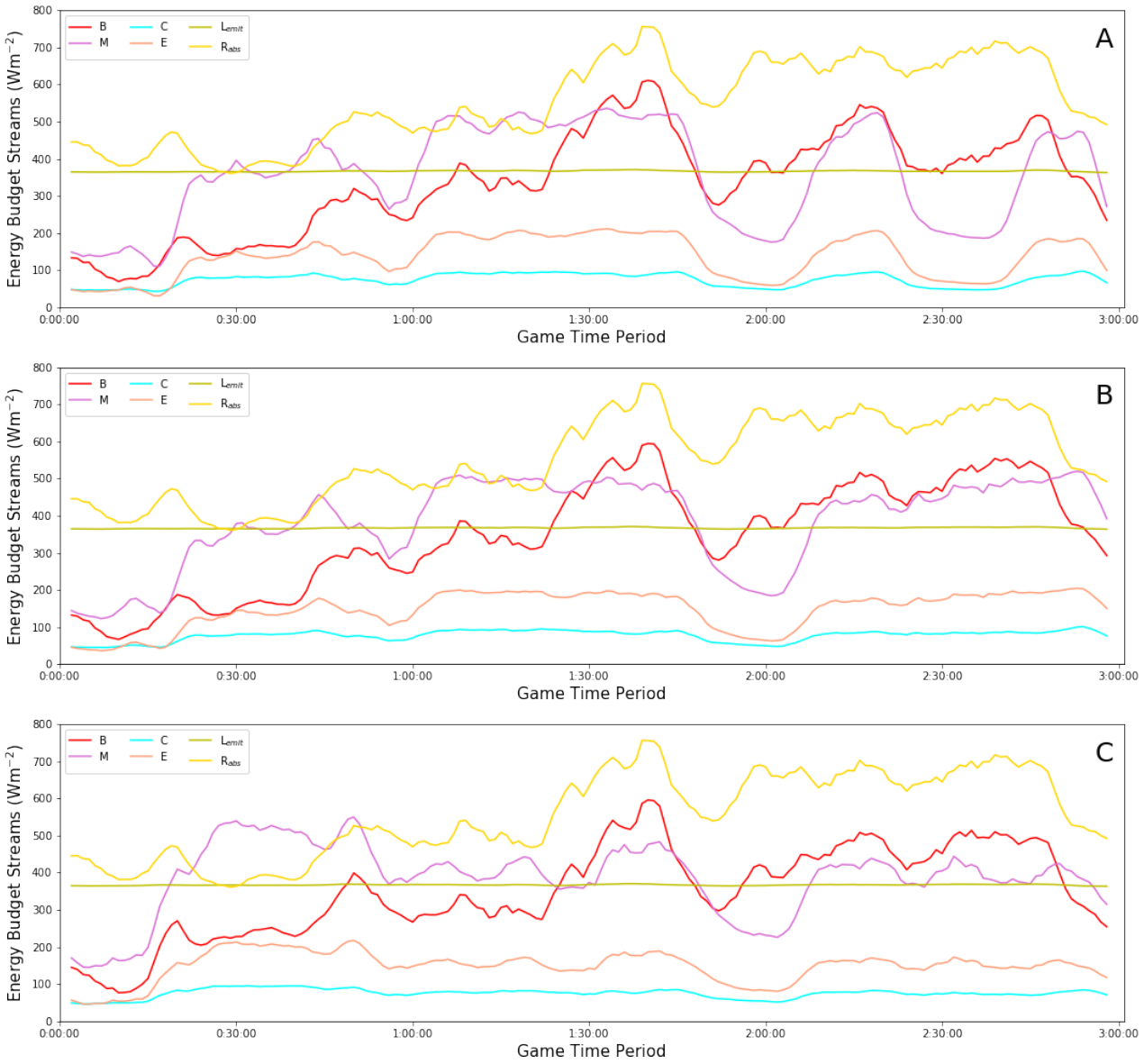

Figure D.2. The EBs (red line) and corresponding EB streams (M (purple line), R_{abs} (yellow line), C (blue line), E (orange line), and L_{emit} (green line)) for A) the midfielder B) the defender, and C) the goalie for the women's gold medal match.

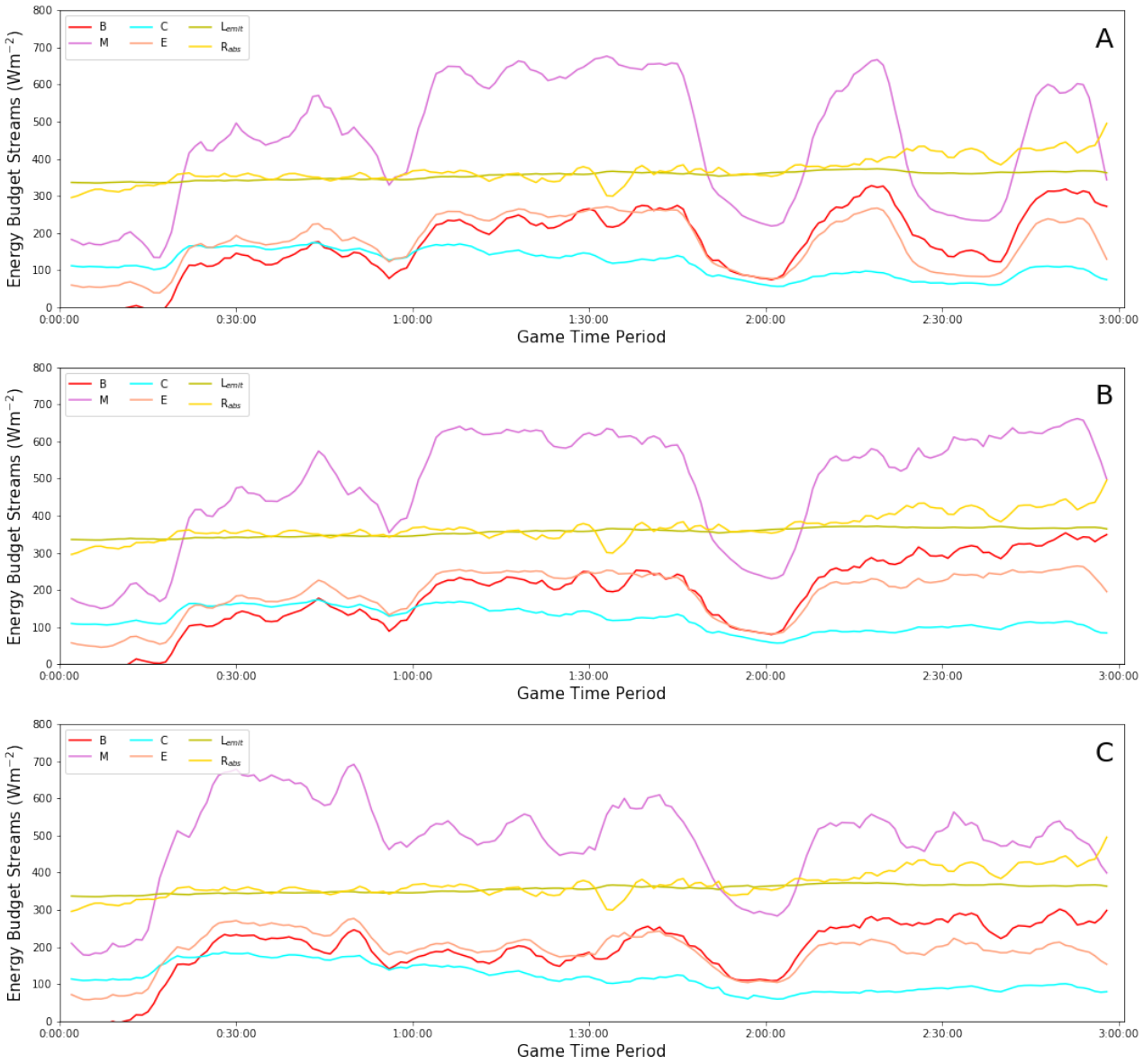

Figure D.3. The EBs (red line) and corresponding EB streams (M (purple line), R_{abs} (yellow line) , C (blue line), E (orange line), and L_{emit} (green line)) for A) the midfielder B) the defender, and C) the goalie for the men's gold medal match.